Physics

SCIENCE OF LIGHT

VOLUME 10 NUMBER 3

December
1961

Published by the

Institute for Optical Research

Tokyo University of Education

in collaboration with

The Spectroscopical Society of Japan

SCIENCE OF LIGHT

Science of Light contains reports of the Institute for Optical Research and contribution from other science bodies about similar subjects

The editorial staff consists of following members:

All communications should be addressed to the director or to the librarian of the Institute.

The Institute for Optical Research

Tokyo University of Education

400, Hyakunin-tyo-4, Shinzyuku-ku, Tokyo, Japan

Printed by
Kabushiki Kaisha Kokusai Insatsu,
Tokyo

Reflectance and Transmittance of Turbid Media

Hirokazu KAWAHATA*

The Electrotechnical Laboratory, Osaka Branch

(Received June 5, 1961)

Abstract

Pure reflectance and transmittance of paint layers (TiO_2, ZnO and $PbCO_3$) as turbid media are measured. ZnO paint layers in particular are investigated in order to measure the reflectance and transmittance as functions of layer thickness and particle concentration. For internal reflectance at the boundary surface between air and the layer, values from 0.3 to 0.6 are found.

1. Introduction

A turbid medium is a system composed of a number of particles suspended in medium. The reflection and transmission depend mainly on the scattering of light by the particles.

Papers have been published on the reflectance and transmmittance of opal glass but as far as the author is aware no study has as yet been made on the transmission of light through thin paint layers in particular on the angular distribution of transmitted light. In this paper, experimental procedures and results of such a study will be described. In a paper that follows, size and refractive index of the particles in the state of paint will be derived from the results obtained in the present work in which the determination of these factors is the main purpose.

2. Experimental Method

1. General Equation

When diffuse light falls on a turbid medium bounded by two parallel plane surfaces, photometrically obtained values of total reflectance and total transmittance contain external and internal reflectances at the boundary surfaces besides pure reflectance and transmittance. Therefore, in order to determine pure reflectance and transmittance, these superfluous factors must be eliminated from the photometric values.

* Now at Research Laboratory, Matsushita Electronics Corporation.

Let ρ and τ be the observed values of total reflectance and transmittance for incident diffuse light. Expressions for ρ and τ in the case of one layer turbid medium are given by Preston[1]:

$$\rho=r_0+\frac{(1-r_0)(1-r_1)[R(1-r_2R)+r_2T^2]}{(1-r_1R)(1-r_2R)-r_1r_2T^2} \tag{1}$$

$$\tau=\frac{(1-r_0)(1-r_2)T}{(1-r_1R)(1-r_2R)-r_1r_2T^2} \tag{2}$$

where R and T are the pure reflectance and transmittance respectively, r_0 is the external reflectance for the incident light and r_1 and r_2 are the internal reflectances for the scattered light at the two boundary surfaces as illustrated in Fig. 1.

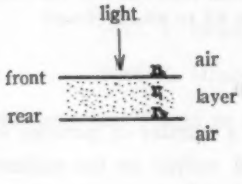

Fig. 1. Model of sample with two boundaries.

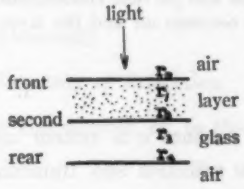

Fig. 2. Model of sample with three boundaries.

Since a layer of paint with no back support is difficult to be prepared, the paint was coated on glass plates, Hence all the samples used for test were double-layered—a glass plate and a paint layer in close contact—and therefore had three boundary surfaces as illustrated in Fig. 2. Thus the formulas corresponding to Eqs. (1) and (2) become:

$$\rho=r_0+\frac{(1-r_0)(1-r_1)}{(1-r_1R)\{1-r_1r_4(1-r_2)(1-r_3)T^2\cdot T_g^2\}}\cdot \left\{R+\frac{(1-r_2)(1-r_3)r_4T^2\cdot T_g^2}{1-r_4R(1-r_2)(1-r_3)T_g^2}\right\}+A(r_2,\,r_3) \tag{3}$$

$$\tau=\frac{(1-r_0)(1-r_2)(1-r_4)T\cdot T_g}{[1-r_1r_4(1-r_2)(1-r_3)T^2\cdot T_g^2][1-r_4R(1-r_2)(1-r_3)T_g^2]}\left\{1+\frac{r_1R}{1-r_1R}\right\}+B(r_2,\,r_3) \tag{4}$$

In Eqs. (3) and (4) the following notations are used.

1) J. S. Preston: Proc. of the International Illumination Congress, 1 (1931) 387.

r_0 : External reflectance of the front surface of paint layer for diffuse light
r_1 : Internal reflectance of the front surface from layer to air
r_2 : Internal reflectance of the second surface from layer to glass
r_3 : Internal reflectance of the second surface from glass to layer
r_4 : Internal reflectance of the rear surface from glass to air
T_g : Transmittance of the glass
$A(r_2r_3)$: Effect on ρ of the inter-reflectance at the second surface
$B(r_2r_3)$: Effect on τ of the inter-reflectance at the second surface

Eqs. (3) and (4) seem to be complicated, but if the optical properties of the medium (clear lacquer) are found to be equal to those of the glass, as will be proved in section IV, then higher order terms in r_1r_4 can be neglected and suffix 4 can now be replaced by 2, and Eqs. (3) and (4) are reduced to Eqs. (1) and (2) on which basis the experiment was carried out.

From Eqs. (1) and (2) we can derive the following expressions

$$R=\frac{l(\rho-r_0)-r_2\tau^2}{l^2-r_2^2\tau^2} \tag{5}$$

$$T=\frac{[l-r_2(\rho-r_0)]\tau}{l^2-r_2^2\tau^2} \tag{6}$$

$$l=1-r_0-r_1(1-\rho)$$

R and T cannot yet be solved from Eqs. (5) and (6) unless more information on unknown r_1, r_2 and r_0 is given

2. External Reflectance r_0

Accurate estimation of r_0 cannot be made experimentally because of the difficulty of measuring r_0 alone without the effects of R. Walsh[2] computed r_0 for specular reflection from Fresnel's formula. For his result to become applicable, samples were prepared by steadily watching the reflection on the surface and taking good care to have them made as similar as possible with one another. According to Walsh, r_0 is 0.092 when perfectly diffuse light falls on a suface of refractive index $n=1.5$

3. Internal Reflectance r_1 and r_2

If a sample is blackened on its back, the transmitted light reaching the rear surface will be absorbed and not come back again to the front surface. Hence the terms involving T in Eq. (1) vanish and Eq. (1) becomes

$$\rho_0=r_0+\frac{(1-r_0)(1-r_1)R}{1-r_1R} \tag{7}$$

2) J.W.T. Walsh: Dept. Sci. Ind. Res. Illumination Research Tech. Pap. 2 (1926) 10.

where ρ_0 is the photometrically obtained value of the total reflectance for the sample. If furthermore it is assumed that the front and rear surface are optically identical, r_1 and r_2 will be equal, and we obtain from Eq. (5) and (7)

$$r_1=r_2=\frac{(1-r_0)(\rho-\rho_0)}{\tau^2+(1-\rho)(\rho-\rho_0)} \tag{8}$$

It seems likely that the values of r_1 and r_2 depend on the incident angle on the surface. The refraction of the incident light, however, will not tell to what extent the scattered light is diffuse, for when the scattered light travels from the layer to the air, the light at incident angles above 42 degrees cannot emerge because of the total reflection and a similar phenomenon will occur at the front surface. Ryde[3] derived an equation for a particular case of $R=T$, from which r_2 could be calculated. But this condition is difficult to be realised, and the use of the experimental method mentioned above becomes inevitable. However it should be noted that this method can be used only in the case when the difference between ρ and ρ_0 is experimentally detectable.

On the other hand, neither r_1 nor r_2 are found explicitly in equations for R and T. On using the relation Eq. (8) in Eqs. (5) and (6) we obtain:

$$R=\frac{(\rho_0-r_0)[\tau^2+(1-\rho)(\rho-\rho_0)]}{(1-r_0)[\tau^2-(\rho-\rho_0)^2]} \tag{9}$$

$$T=\frac{[\tau^2+(\rho-\rho_0)(r_0-\rho)][\tau^2+(1-\rho)(\rho-\rho_0)]}{\tau(1-r_0)[\tau^2-(\rho-\rho_0)^2]} \tag{10}$$

Consequently the pure reflectance and transmittance can be obtained from Eqs. (9) and (10) by the use of photometric values and approximate value of r_0. It is not necessary to know the values of r_1 and r_2, but it is still a matter of interest to check what these values become.

3. Apparatus for Experiment

In order to measure the pure reflectance and transmittance of a turbid medium and the angular distribution of transmitted monochromatic light, the following measuring arrangement was used.

(1) Monochromator
(2) Goniophotometer
(3) Ulbricht spheres
(4) Detector devices, etc.

3) J. W. Ryde: Proc. Roy. Soc. (London) A 131, 817 (1931) 451.

Fig. 3 shows the general view of the apparatus and Fig. 4 its schematic representation. The detail of the apparatus will be described below.

Fig. 3. General view of the apparatus: Monochromator and Goniophotometer are in the central part, light source and Ulbricht spheres are on the left, and detector devices are on the right.

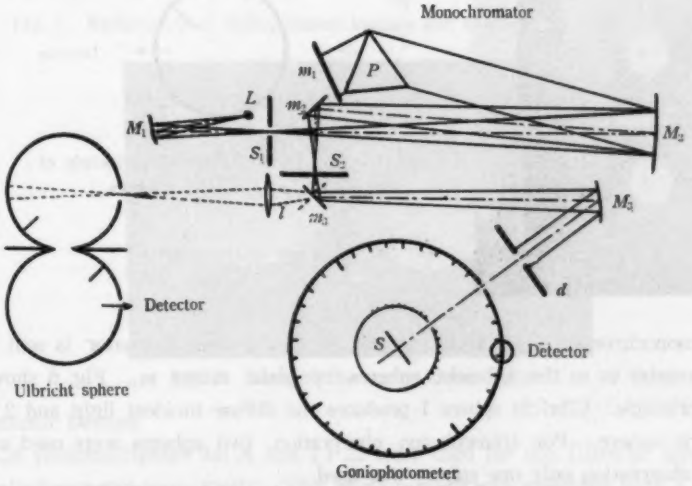

Fig. 4. Schematic representation of the apparatus.
L: light source; m_1, m_2 and m_3: plane mirrors; M_1, M_2 and M_3: spherical mirrors; l: lens; S_1 and S_2: slits; d: diaphram; S: support of sample.

(1) Monochromator

As seen in Fig. 4, the monochromator is of a usual type with a 60° glass prism, Littlow mirror and collimator mirror of $f=8$.

(2) Goniophotometer

This equipment was used to observe the angular distribution of transmitted light and the specular reflectance. It is composed of support S of the sample and a manually or mechanically rotated detector with a range from 0 to 360 degrees around the center of the sample.

(3) Ulbricht Spheres

Fig. 5 shows a view of the spheres. Generally, it is said that an artificially diffuse light of perfect uniformity is very difficult to be obtained, but the method of utilizing inter-reflection on the inside walls of Ulbricht sphere has been in frequent use to realize the diffuse light. In this experiment, two Ulbricht spheres were used to observe the total transmittance for monochromatic diffuse light.

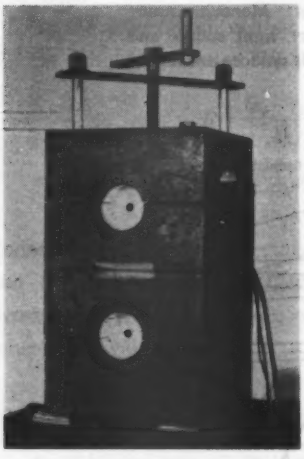

← Fig. 5. View of the spheres.

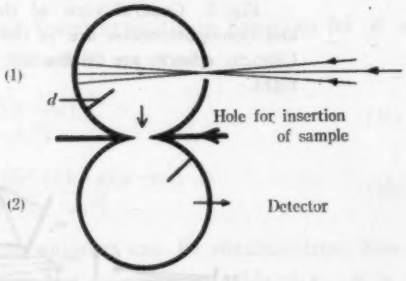

↑ Fig. 6. Working principle of the spheres.

The monochromatic light from exit slit S_2 of the monochromator is sent to the goniophotometer or to the Ulbricht spheres by plane mirror m_3. Fig. 6 shows the working principle. Ulbricht sphere 1 produces the diffuse incident light and 2 is the photometric sphere. For transmission observation, two spheres were used and for reflection observation only one sphere was used.

Preparation of Ulbricht spheres—The spheres were made of Aluminum casting with $BaSO_4$ coated inner walls. The inner diameter was 150 mm, the diameter of the hole for observation 10 mm and the diameter of the aperture for insertion of sample

20 *mm*. The specific reflectance of a $BaSO_4$ coated surface in comparison with a fresh magnesium oxide coated surface is shown in Fig. 7. Fig. 8 shows the coated inner walls.

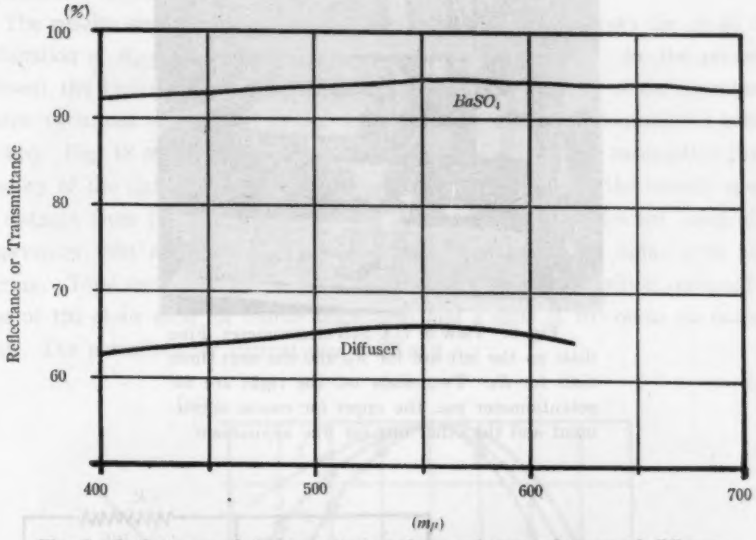

Fig. 7. Reflectance of $BaSO_4$ coated surface and transmittance of diffuser.

Fig. 8. View of the coated inner walls.

(4) Detector Devices

RCA photomultipliers 931 *A* and 1 *P* 22 were used for the Ulbricht spheres and the goniophotometer respectively. The photo-current was measured with a *UX*-54 *B* electrometer (Fig. 9). The electrical circuit of this electrometer is the Barth's one[4]

4) G. Barth: Zeits. f. Physik, **87** (1934) 399.
H. Ezoe: Shitsuryo Bunseki, **3** (1954) 41, **4** (1955) 53, **5** (1955) 52.

which is shown in Fig. 10. From the many available tubes, photomultiplier tubes 931 *A* and 1 *P* 22 were chosen as the most stable tubes for this circuit. Twenty five

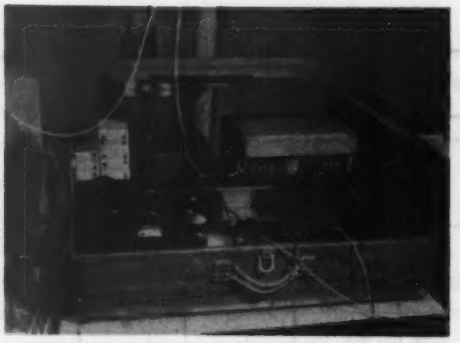

Fig. 9. View of *UX*-54*B* electrometer. Five dials on the left are for R_p and the next three dials for R_s. Two dials on the right are for potentiometer use, the upper for coarse adjustment and the other one for fine adjustment.

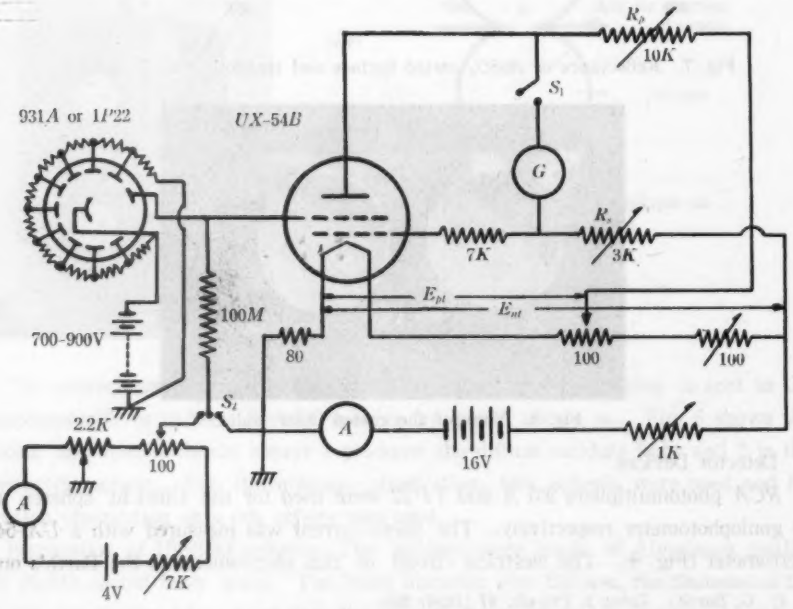

Fig. 10. Electrometer circuit.

years ago when the electrometer was first made by Seki[5], it had Soller's circuit which was now replaced by another one to suit to the present use. The stability of the circuit was checked by Du-Bridge's method of representing the galvanometer current as a function of the filament current.

The results are shown in Fig. 11. The appended table shows the detail of the combination of E_{pt} (Volt), E_{nt} (Volt), R_p (kohms) and R_s (kohms. In the present experiment, the 3 rd combination was adopted. Linearity of reading of the potentiometer against variations of intensity of the light incident on the photomultiplier tube was checked. Fig. 12 shows the result. This test was made on the assumption that the intensity of the light incident on the detector is proportional to the inverse spuare of the distance from the light source to the detector. An incandescent lamp of color temperature 2854°K as the light source, red, blue and green lights were used by filtering. Total resistance of the potentiometer was 2300 ohms which consisted of 22 steps of 100 ohms each for coarse adjustment and a slide of 100 ohms for finl adjustment. The potentiometer current was 0.435 mA.

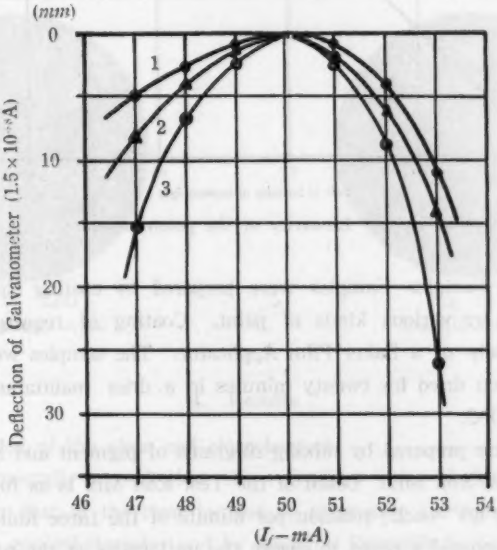

Curve	E_{pt}	E_{nt}	R_p	R_s
1	13.6	10.8	17.1	9.95
2	12.2	10.7	9.01	5.20
3	10.4	11.7	3.36	2.00

Fig. 11. Stability characteristics of the electrometer.

5) S. Seki, T. Ogawa and K. Tsurui: Bulletin of Elect. Tech. Lab. 8 (1934) 207.

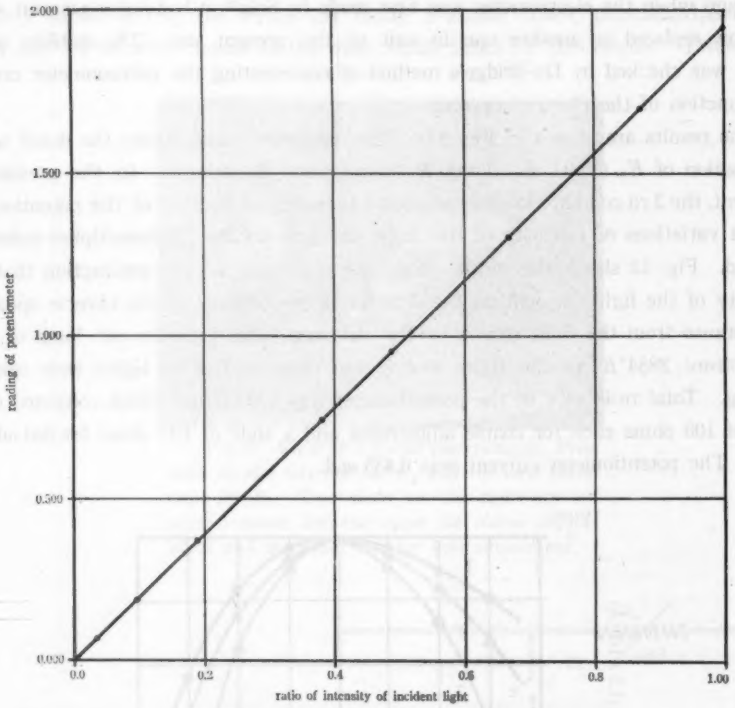

Fig. 12. Linearity of the potentiometer.

Preparation of Samples—Samples were prepared by coating clear washed photographic dry plates by various kinds of paint. Coating of required thickness was made with the help of a Baker Film Applicator. The samples were left in air for about one hour then dried for twenty minutes in a drier maintained at a constant temperature of 120°C.

The paints were prepared by mixing 20 grams of pigment and 80 grams of clear lacquer with a Test Roll Mill. Detail of the Test Roll Mill is as follows. Diameters of the three Rolls: 6.5″ each; rotation per minute of the three Rolls: 150, 50 and 25.

Mixing was repeated 6 times to assure the uniformity of the paint, and a small amount of thinner was added to facilitate easy spread of the paint. The paint was then passed through a 325 mesh sieve to doubly assure its uniformity. Because of the evaporation of used thinner, decrease of the prepared thickness of paint layer when thoroughly dried could not be avoided. Chief constituent of the lacquer used for the paint was refined linseed oil.

Fig. 13, 14, 15 and 16 show microscopical photographs of typical samples, They justify the assumption that the pigments diffuse to a satisfactory uniformity in the medium. They show the difference in size of pigment particles by different paints, the size increasing in the sequence TiO_2 (Anatase), TiO_2 (Rutile), ZnO and $PbCO_3$.

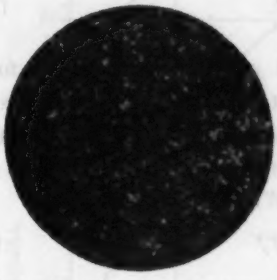

Fig. 13. TiO_2 (Anatase type)
magnification: ×960.

Fig. 14. TiO_2 (Rutile type)
magnification: ×960.

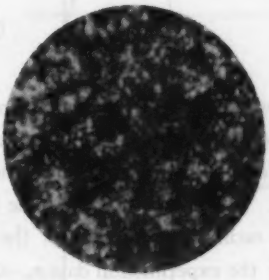

Fig. 15. ZnO
magnification: ×960

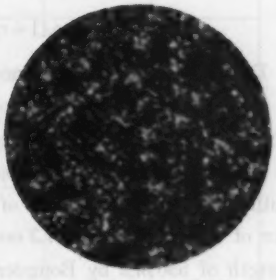

Fig. 16. $PbCO_3$
magnification: ×960

4. Results

(1) Refractive index of the glass and clear lacquer

It was experimentally proved that the refractive index of the glass was approximately equal to that of the clear lacquer by measuring the reflectance and transmittance with the goniophotometer and by applying Fresnel's formula to the results. Hence it was confirmed that the reflection at the boundary surface between the glass and layer could be neglected. Consequently, Eqs. (1) and (2) could be used instead of Eqs. (3) and (4).

When non-polarized monochromatic light is incident at angle i on glass of refractive index n, reflectance ρ_g is given by Fresnel's formula as follows

$$\rho_g=\frac{1}{2}(\rho_{g\parallel}+\rho_{g\perp}) \tag{11}$$

$$\rho_{g\parallel}=\left|\frac{\cos i-\sqrt{n^2-\sin^2 i}}{\cos i+\sqrt{n^2-\sin^2 i}}\right|^2 \tag{12}$$

$$\rho_{g\perp}=\left|\frac{n^2\cos i-\sqrt{n^2-\sin^2 i}}{n^2\cos i+\sqrt{n^2-\sin^2 i}}\right|^2 \tag{13}$$

where $\rho_{g\parallel}$ is the reflectance for parallel component and $\rho_{g\perp}$ the reflectance for perpendicular component with respect to the plane of incidence. When the external reflection at the front surface and the effect of the internal reflection at the boundary surface are taken into account, photometric reflectance r_g and transmittance τ_g of the glass for monochromatic incident light are expressed as follows

$$r_g=\rho_g+\rho_g(1-\rho_g)^2\cdot T_g^2/1-\rho_g^2T_g^2 \tag{14}$$

$$\tau_g=T_g\cdot(1-\rho_g)^2/1-\rho_g^2\cdot T_g^2 \tag{15}$$

Combination of Eqs. (14) and (15) yields

$$r_g=\rho_g(1+\tau_g\cdot T_g) \tag{16}$$

where T_g is the true transmittance of the glass.

In an experiment with light of 550 $m\mu$ wave-length, r_g and τ_g for an incident angle of 7.5 degrees were measured with the goniophotometer, and T_g was measured with a Hitachi's recording spectrophotometer. Curve (1) in Fig. 17 shows the true transmittance of a glass plate of 10 mm thickness. From curve (1) the true transmittance of a glass plate of 1.3 mm thickness was estimated at 0.998 for the same wave-length of 550 $m\mu$ by Bouguer's law. By using the experimental data $r_g=0.0806$, $\tau_g=0.916$ and $T_g=0.998$ in Eq. (16), $\rho_g=0.0421$ was obtained. From Eqs. (11), (12) and (13), $n=1.52$ was found for the refractive index of the glass. A similar experiment was made on the clear lacquer with a sample made of a glass plate coated with a layer of the lacquer. Then we have the expression

$$r_l=\rho_l+\rho_g\cdot\tau_l\cdot T_g\cdot T_l(1-\rho_l)/1-\rho_g \tag{17}$$

where

r_l: Photometric reflectance
ρ_l: True reflectance of the clear lacquer
T_l: True transmittance of the clear lacquer

In derivation of Eq. (17), reflection at the boundary surface between the glass and the clear lacquer was neglected as the first approximation. Although this is exactly what we are going to prove, the result will show that the assumption is

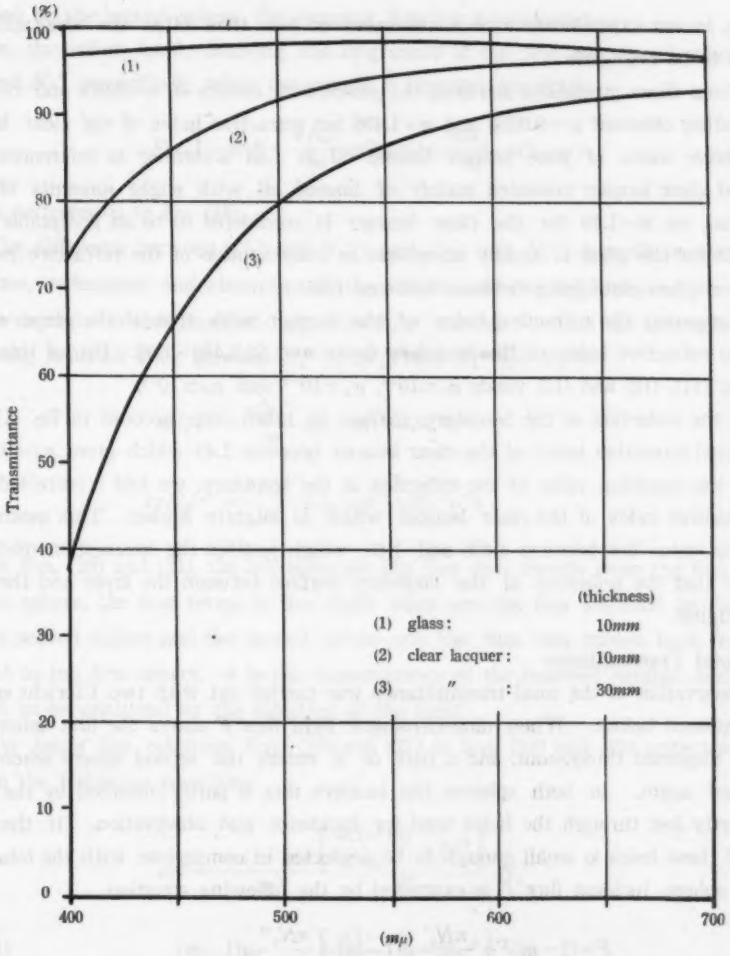

Fig. 17. Spectral transmittance curves of the glass plate and the clear lacquer.

justified.

The values of ρ_g and T_g are obtained in Eq. (16) and the value of T_l is easily found to be nearly equal to 1 from curves (2) and (3) in Fig. 17. Curves (2) and (3) in Fig. 17 show the true transmittance of the clear lacquer layer of which the thickness is 10 *mm* and 30 *mm* respectively. Bouguer's law was found to hold sufficiently between curves (2) and (3). Absorption coefficient of the clear lacquer was estimated at 0.31 for a light of wave-length 400 *mμ* where the strongest absorption occurs,

hence, in our experiments with a thickness of less than 60 μ, the absorption was found to be negligible.

From these procedures and from the photometric results of $r_l=0.078$ and $\tau_l=0.917$, the author obtained $\rho_l=0.0386$ and $n=1.486$ for refractive index of the clear lacquer. Refractive index of pure refined linseed oil is 1.48 according to references. The present clear lacquer consisted mainly of linseed oil with slight amounts of other material, so $n=1.49$ for the clear lacquer is considered to be an acceptable value. $n=1.52$ for the glass is equally acceptable in consideration of the refractive index of common glass plate lying between 1.51 and 1.53.

Comparing the refractive index of the lacquer with that of the glass, we find for the refractive index at the boundary layer $n=1.52/1.486=1.02$. Use of this value in Eqs. (11), (12) and (13) yields $\rho_{\parallel}\simeq 10^{-4}$, $\rho_{\perp}\simeq 10^{-4}$ and $\rho_{gl}\simeq 10^{-4}$.

If the reflection at the boundary surface is taken into account in Eq. (17), the calculated refractive index of the clear lacquer becomes 1.49 which gives $\rho_{gl}=0.00025$. Using the resulting value of the reflection at the boundary, we find a corrected value of refractive index of the clear lacquer which is slightly higher. This means that the true value lies between 1.486 and 1.49, which justifies the assumption made previously that the reflection at the boundary surface between the layer and the glass is negligible.

(2) Total Transmittance

Observation of the total transmittance was carried out with two Ulbricht spheres as mentioned before. When monochromatic light flux F enters the first sphere, the flux is dispersed throughout, and a part of it enters the second sphere where it is dispersed again. In both spheres the incident flux is partly absorbed by the walls and partly lost through the holes used for incidence and observation. If the total area of these holes is small enough to be neglected in comparison with the total area of the sphere, incident flux F is expressed by the following equation

$$F=(1-m)F+\frac{\pi N_0'}{m}a(1-m)+\frac{\pi N_0''}{m}a(1-m) \tag{18}$$

where m is the reflectance of the walls of the sphere. N_0' and N_0'' are respectively the brightness of the first and second spheres, when the sample is not inserted in the test aperture. If c'' is the ratio of the area of the spherical cap of the test aperture to the total area of the sphere, $a=1-c''$ indicates the rest of the area of the sphere by taking the total area of the sphere as unity.

The first term of the right side of Eq. (18) is the quantity absorbed by the walls of the first sphere from the incident flux, the second term the quantity absorbed by the walls of the first sphere from the reflected flux and the third term the quantity

absorbed by the second sphere, the escaping flux being neglected.

On the other hand, denoting the brightness of the first and second spheres by N_x' and N_x'' respectively when the sample is inserted, we obtain

$$F=(1-m)F+\frac{\pi N_x'}{m}a(1-m)+\frac{\pi N_x''}{m}a(1-m) \tag{19}$$

which corresponds to Eq. (18).

The difference between (N_x' and N_x'') and (N_0' and N_0'') depends on the transmittance, reflectance and absorption of the sample. As the brightness of the second sphere depends on the dispersed light flux $N_0'c''$ (or $N_x'c''$) from the first sphere, the following relations exist between N_0' (or N_x') and N_0'' (or N_x'').

$$\pi N_0'c''=\frac{\pi N_0''}{m}a(1-m)+\pi N_0''c'' \tag{20}$$

$$k\pi N_x'c''=\frac{\pi N_x''}{m}a(1-m)+\pi N_x''c''k \tag{21}$$

In Eqs. (20) and (21), the left sides are the flux that travels from the first to the second sphere, the first terms of the right sides are the flux absorbed by the walls of the second sphere and the second terms are the flux that travels back from the second to the first sphere. k is the transmittance of the inserted sample and is assumed to be unaltered by the direction of the light.

On using the relations Eqs. (20) and (21) in Eqs. (18) and (19) respectively, we obtain the following equations

$$mF=\frac{\pi a(1-m)}{m}\frac{\left[\frac{a(1-m)}{m}+2c''\right]}{c''}\cdot N_0'' \tag{22}$$

$$mF=\frac{\pi a(1-m)}{m}\frac{\left[\frac{a(1-m)}{m}+2kc''\right]}{kc''}\cdot N_x'' \tag{23}$$

From Eqs. (22) and (23) we have the following relation by putting $N_x''/N_0''=A$

$$k=A\cdot\frac{1}{1+\frac{2mc''(1-A)}{a(1-m)}} \tag{24}$$

Eq. (24) gives the transmittance k as a function of the photometrically observed value A (apparent transmittance).

(3) Total Reflectance

Taylor[6] and Preston[7] gave reports on their measurements of total reflectance of MgO-surface for diffuse light. Both authors used the Ulbricht sphere. The method they used was applied in the present experiments. The structure of the sphere is similar to that of the sphere used for the measurement of transmittance except for the size. On consideration of the accuracy of the method and the limited sensitivity of the detecting devices, the sphere was made in the following dimensions.

Radius of the sphere: 30 *mm*.

Ratio c' of the plane area of the test aperture to the total area of the sphere: 0.024.

Ratio c'' of the area of the spherical cap screening the test aperture to the total area of the sphere: 0.025.

Ratio d' of the plane area of the hole for observation to the total area of the sphere: 0.007.

Ratio d'' of the area of the spherical cap for observation hole to the total area of the sphere: nearly equal to d'.

Rest of the area a of the sphere: $1-c''-d''$ (total area is taken as unity)

The area of the hole for illumination being sufficiently small, it was neglected.

Let F be the flux entering through the illuminating hole, b_0 be the brightness of the sphere with the test aperture covered by a black box and pF_0 be the flux escaping through the observing hole. Then we obtain the following equation:

$$F=(\pi b_0 c''+c'mF)+pF_0+\left(\frac{\pi b_0}{m}a+F\right)(1-m) \tag{25}$$

where m is the reflectance of the walls of the sphere which are coated with smoked magnecium. The coating was made to such an extent that the irregularity of the base surface vanished. Coatings were not sufficient: m was lower than the instrinsic reflectance of the MgO surface as shown later.

When a sample of reflectance m_x is placed at the test aperture, Eq. (25) becomes as follows:

$$F=(\pi b_x c''+c'mF)(1-m_x)+pF_x+\left(\frac{\pi b_x}{m}a+F\right)(1-m) \tag{26}$$

where b_x is the brightness of the walls of the sphere with the sample of the reflectance m_x at the test aperture, pF_x is the flux escaping through the observing hole, p being the transmittance of the diffuser for the diffuse incident light fixed at

6) A. H. Taylor: J. Opt. Soc. Am. **4** (1920) 9.
7) J. S. Preston: Trans. Opt. Soc. **31** (1929) 15.

the observing hole. p was measured by the method mentioned in the preceding section and the data are given in Fig. 7.

On the other hand, for F_0 and F_x we have the following relations

$$F_0=d'(\pi b_0+mF) \tag{27}$$

$$F_x=d'(\pi b_x+mF) \tag{28}$$

Using the relations of Eqs. (27) and (28) in Eqs. (25) and (26), we obtain the following equations

$$b_0=\frac{m^2F(1-p\,d'-c')}{\pi\{m(c''+p\,d')+(1-m)a\}} \tag{29}$$

$$b_x=\frac{m^2F(1-p\,d'-c'+c'm_x)}{\pi\{(1-m_x)mc''+mpd'+(1-m)a\}} \tag{30}$$

Furthermore, use of these b_0 and b_x in Eqs. (27) and (28) respectively, gives

$$F_0=d'mF\frac{(d'+c'')m+a}{(c''-a+p\,d')m+a} \tag{31}$$

$$F_x=d'mF\frac{\{d'+c''+(c'-c'')m_x\}m+a}{(1-m_x)mc''+mp\,d'+(1-m)a} \tag{32}$$

Then the photometrically observed value K_x is given by

$$K_x=\frac{pF_x}{pF_0}=\frac{[\{d'+c''+(c'-c'')m_x\}m+a][(c''-a+p\,d')m+a]}{[(1-m_x)mc''+mp\,d'+(1-m)a][(d'+c'')m+a]} \tag{33}$$

In order to obtain the reflectance m_x of a sample by the use of Eq. (33), the value of m must be known. To this purpose, K_x was measured first with a sample of known reflectance, and from the value of K_x thus found, m was computed.

As a standard of such reflectance, MgO surface with its reflectance given in American Institute of Physics Handbook was adopted. Among a number of MgO surfaces prepared by the method given in JIS Z 8722, one that had the highest reflectance was used as the standard. According to authentic literature, reflectance of MgO surface is 0.99, 0.98 and 0.97 for 600, 500 and 400 $m\mu$ respectively. By interpolation, reflectance for 450 and 550 $m\mu$ was found as 0.975 and 0.985 respectively, and with these values used in Eq. (33) together with the values of K_x obtained photometrically at 400, 450, 500, 550 and 600 $m\mu$, values of m for the above wavelengths were obtained as 0.932, 0.933, 0.934, 0.934 and 0.935 respectively. With these values used in Eq. (33), the total reflectance of the sample was found.

(4) Pure Reflectance and Transmittance

Using the photometric results of the above mentioned experiments in Eqs. (9)

and (10), we obtain the pure reflectance R and transmittance T of the paint layers which are shown in Fig. 18. Full curves are for the pure reflectance R and dotted curves the pure transmittance T. Number on the curves in Fig. 18 correspond to those in Fig. 20. The fact that R decreases and T increases as the wave-length becomes longer shows that the effect of light scattering by the particles in the medium is considerable. This scattering effect is easily understood from the results of obser vations made on the angular distribution of transmitted light shown in Fig. 21~24. These results depend on the quality and quantity of particles contained in the medium which will be the subject of a later report. Fig. 19 shows R and T for various layers

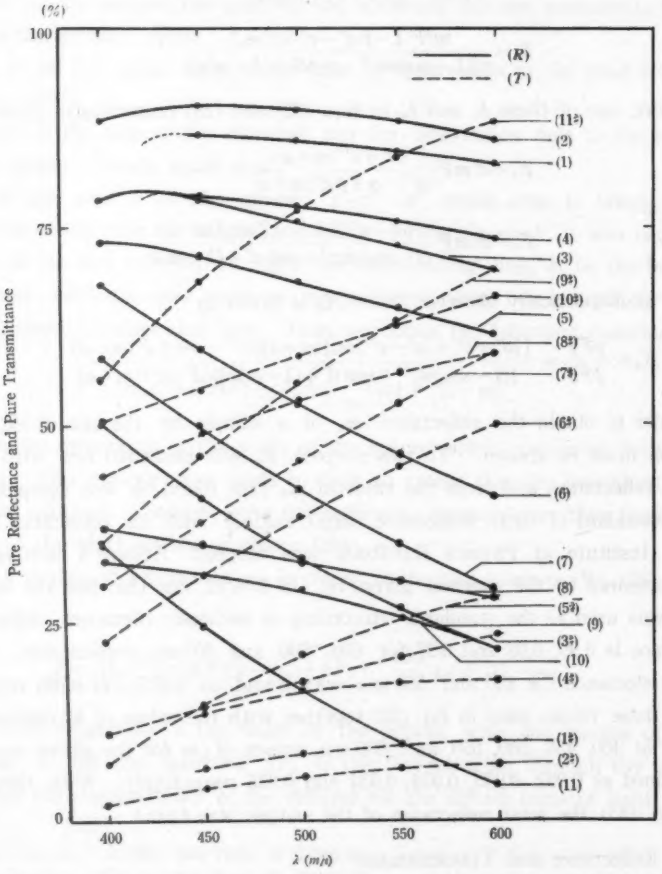

Fig. 18. Pure reflectance and transmittance of ZnO, TiO_2, and $PbCO_3$.

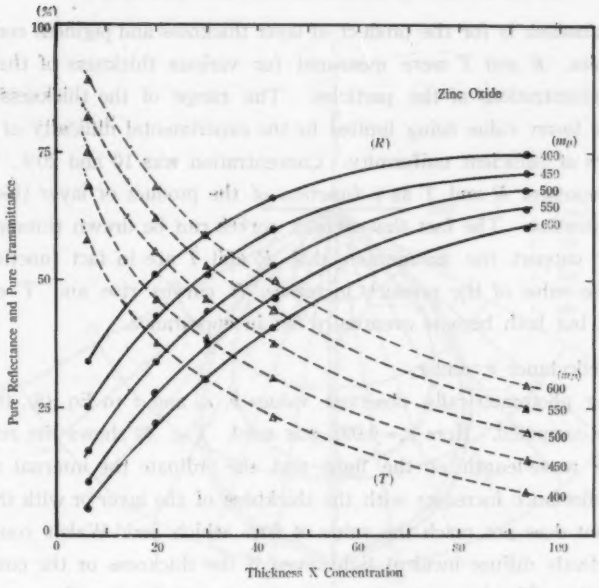

Fig. 19. R and T of ZnO layers of various thickness and pigment concentration.

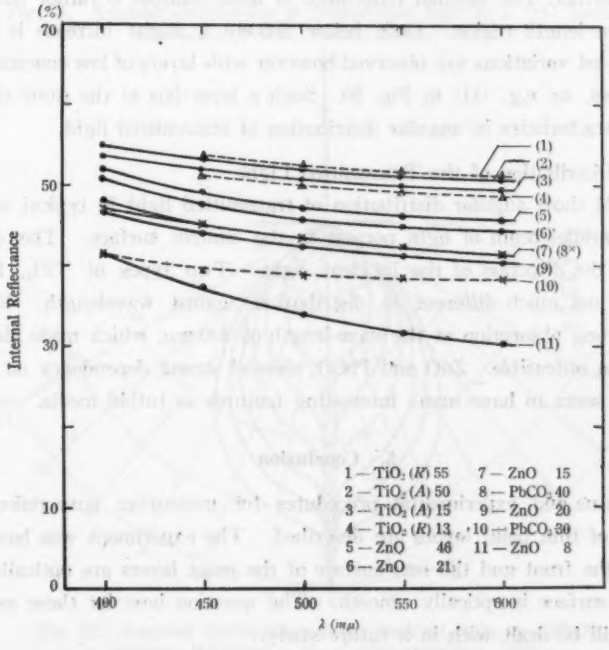

Fig. 20. Internal reflectance of various samples.

of ZnO. The abscissa is for the product of layer thickness and pigment concentration in arbitrary units. R and T were measured for various thickness of the layer and for different concentrations of the particles. The range of the thickness was from $8\,\mu$ to $60\,\mu$, the lower value being limited by the experimental difficulty of producing very thin layers of sufficient uniformity. Concentration was 10 and 20%. It seemed reasonable to represent R and T as a function of the product of layer thickness and pigment concentration. The fact that smooth curves can be drawn through 5 plotted points seems to support the assumption that R and T are in fact functions of this product. As the value of the product increases, R curves rise and T curves fall steeply at first, but both become eventually flat in appearance.

(5) Internal Reflectance r_1 and r_2

By applying photometrically observed values ρ, ρ_0 and τ to Eq (8), the internal reflectance was computed. Here $r_0=0.092$ was used. Fig. 20 shows the results. The abscissa is the wave-length of the light and the ordinate the internal reflectance. The internal reflectance increases with the thickness of the layer or with the pigment concentration but does not reach the value of 60% which Judd-Walsh computed for the case of perfectly diffuse incident light even if the thickness or the concentration is increased further. The internal reflectance of most samples is rather constant over the whole wave-length region. Only below $500\,m\mu$ a slight increase is noticeable. More pronounced variations are observed however with layers of low concentration and small thickness, as e.g. (11) in Fig. 20. Such a layer has at the same time strong directional characteristics in angular distribution of transmitted light.

(6) Angular Distribution of the Transmitted Light

Fig. 21~24 show angular distribution of transmitted light in typical samples by incidence of parallel beam of light normal to the sample surface. The curves are normalized at the direction of the incident light. Two types of TiO_2, Rutile and Anatase, were not much different in distribution against wavelength. Rutile type has a very strong absorption at the wave-length of $400\,m\mu$, which made the distribution observation unfeasible. ZnO and $PbCO_3$ showed strong dependency on the wavelength. They seem to have many interesting features as turbid media.

5. Conclusion

An apparatus and experimental procedures for measuring pure reflectance and transmittance of thin paint layers are described. The experiment was based on two assumptions: the front and the rear surface of the paint layers are optically identical and the front surface is optically smooth. The question how far these assumptions are justified will be dealt with in a future study.

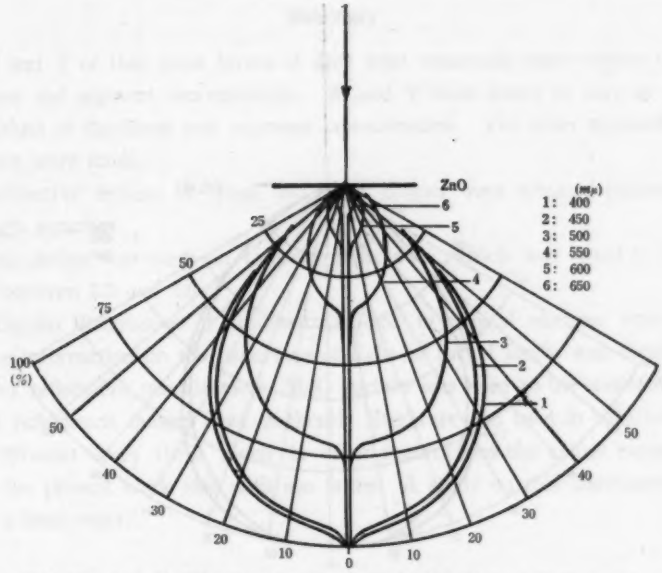

Fig. 21. Angular distribution of transmitted light in a ZnO sample; thickness: 15 μ; concentration: 20%.

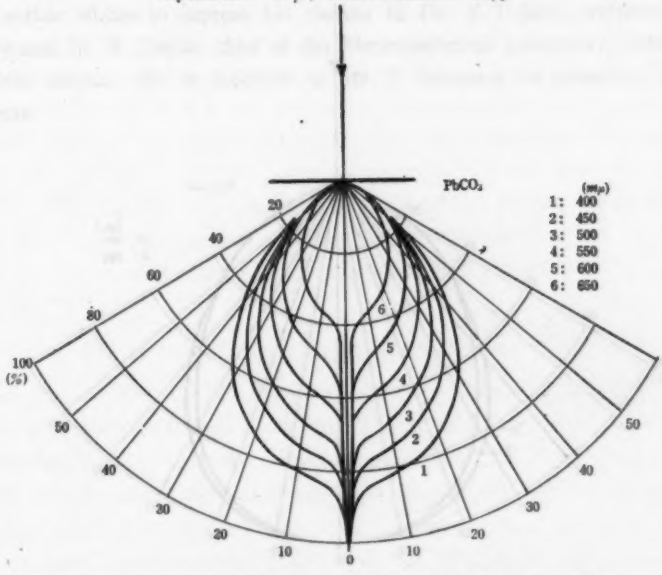

Fig. 22. Angular distribution of transmitted light in a $PbCO_3$ sample; thickness: 30 μ; concentration: 20%.

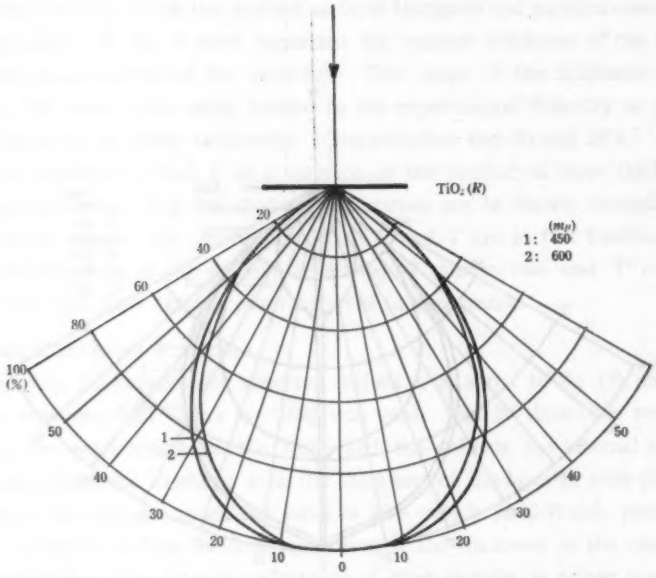

Fig. 23. Angular distribution of transmitted light in a TiO_2 sample (Rutile type); thickness: 13 μ; concentration: 20%.

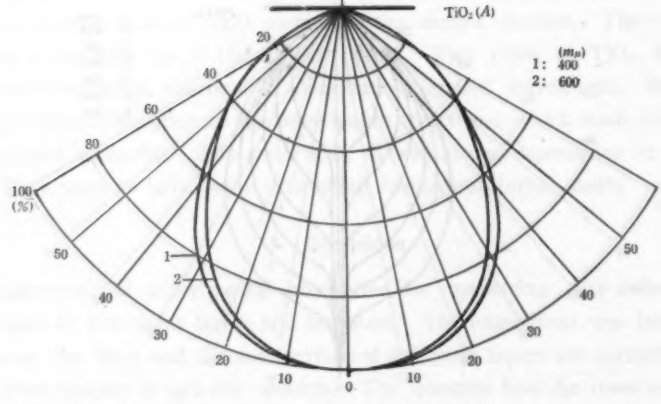

Fig. 24. Angular distribution of transmitted light in a TiO_2 sample (Anatase type); thickness: 15 μ; concentration: 20%.

Summary

1. R and T of thin paint layers of ZnO were measured under various conditions of thickness and pigment concentration. R and T were found to vary as functions of the product of thickness and pigment concentration. For other pigments similar experiments were made.

2. Refractive indices of glass and clear lacquer were obtained photometrically with a high accuracy.

3. Calculation was made on internal reflectance which was found to be approximately between 0.3 and 0.6.

4. Angular distribution of transmitted light in typical samples was observed. Suggestive information on the behaviour of light in turbid media was obtained.

5. For reflectance measurement, MgO surface was used as the standard reflector. Values of reflectance, quoted from authentic literature and used in calculation, seem slightly different from those given in other reports and the values experimentally found in the present work side with the latter. A study on this discrepancy will be given in a later report.

6. Acknowledgement

The author wishes to express his thanks to Dr. Y. Uchida, professor of Kyoto University and Dr. K. Okada, chief of the Electrotechnical Laboratory, Osaka Branch, for valuable advise. He is indebted to Mr. T. Satsutani for assistance during the experiments.

Size and Refractive Index of Particles in Paint Layers

Hirokazu KAWAHATA

Research Laboratory, Matsushita Electronics Corporation

(Received July 15, 1961)

Abstract

The size and refractive index of particles (TiO_2 and ZnO) constituting paint layers are derived from the reflectance and transmittance of the layers. The particle sizes of TiO_2 (Rutile type), TiO_2 (Anatase type) and ZnO are found about 0.3 μ, 0.3 μ and 0.8 μ, and the refractive indices about 2.6, 2.4 and 1.9. respectively.

1. Introduction

In 1931 Ryde[1] integrated Rayleigh's scattering coefficient over all directions of space and derived expressions for the relation of this over-all coefficient to the reflectance and transmittance of turbid medium. These expressions can be used for calculation of the size and refractive index of particles suspended in a medium, provided the reflectance and transmittance are known. Ryde used this method for opal glasses. In the present investigation the method was applied to thin paint layers. In the previous paper, measuring techniques for the evaluation of reflectance and transmittance of such turbid media were discussed in detail. The object of this paper is to derive the particle size and refractive index from Ryde's tables. It was found that the size and refractive index, the size in particular, of the particles in the state of paint layers can be determined photometrically with appreciable accuracy and in good agreement with the result of examination under microscope.

2. Method of Calculating the Size and Refractive Index

Ryde integrated Rayleigh's scattering coefficient over all directions of space and tabulated values of $(F+B)/B, (F'+B)/(F+B)$ and B/E as a function of α which represents characteristic of the particle in a turbid medium. Here F and B are the amounts of light scattered in forward and backward directions respectively when the

1) J. W. Ryde: Proc. Roy. Soc. (London) A 131, (1931) 451.

incident light is diffuse and F' is the amount of light scattered in forward direction when the incident light is of a parallel beam. α and E have the following relations

$$\alpha=\pi Dn_0/\lambda, \qquad E=\pi D^2\eta/16$$
$$\eta\fallingdotseq[(n/n_0)^2-1]^2 \tag{1}$$

where D denotes diameter of a particle, λ wave-length of light, n_0 refractive index of the medium and n refractive index of the particle.

He furthermore showed expressions for the calculation of $(F+B)/B$ and $(F'+B)/(F+B)$ from the reflectance and transmittance of a turbid medium and calculated particle size D and number N of particles per unit volume for opal glasses. To explain briefly this process, values of $(F+B)/B$ or $(F'+B)(F+B)$ are first calculated by the following relations

$$\left.\begin{aligned}\frac{F+B}{B}&=\frac{1}{NB}(q-\mu)\\ \tau_p&=\frac{(1-r_0)^2e^{-qX}}{(1-r_0^2e^{-2qX})}\end{aligned}\right\} \tag{2}$$

$$\frac{\tau'}{\tau}=\frac{1-r_0}{1-r_1}\left\{r_2+(1-r_2)\frac{F'+B}{F+B}\right\} \tag{3}$$

where τ_p is the amount of parallel beam of the transmitted light when a parallel light falls on a turbid medium. r_0 and r_1 are the reflectances of the front surface for the incident parallel light and that for the diffuse light respectively and r_2 the internal reflectance. τ' and τ are the total transmittance of the turbid medium for the incident parallel light and that for the diffuse light respectively. X is thickness of the turbid medium.

Values of α and B/E corresponding to $(F+B)/B$ or $(F'+B)/(F+B)$ can be found in tables. Hence we can calculate D and N or n from $\alpha=\pi Dn_0/\lambda$, $E=\pi D^2\eta/16$ and a well-known fundamental relation between the pure reflectance R and transmittance T of a turbid medium

$$T^2=(1-R)^2-2R\mu/NB \tag{4}$$

Eq. (3) is used only when absorption coeffcient μ of the turbid medium is small compared with scattering term $N(F+B)$.

In the present work, the size and refractive index of particles in paint layer are calculated by applying Ryde's method to the reflectance and transmittance of the paint layer obtained in the previous paper (Part I). Ryde calculated the particle number N from known refractive index n, but in the present work, n was calculated from N which was obtained by calculation based on the particle concentration of the

paint layer by using the values of specific gravities of particles and medium (clear lacquer) taken from the reference[2], the particles being assumed to be spherical. Particles used were white pigments, hence the absorption coefficient μ of the samples was considered small in comparison with $N(F+B)$. Therefore calculations were made mainly by $(F'+B)/(F+B)$. This condition however was not assured to hold always for samples of low particle concentration or very thin layers; observation was made in advance on the angular distribution of penetrated light of parallel incident light to decide which of $(F+B)/B$ and $(F'+B)/(F+B)$ should be used for calculation. The penetrated light in samples of very thin layer or low particle concentration is considerably directional: parallel beam increases and diffuse part represented by the scattering term decreases with increasing directionality. Hence $(F+B)/B$ is easily calculated from the amount of the parallel beam. For ZnO, both $(F+B)/B$ and $(F'+B)/(F+B)$ were used according to the state of the sample, and the comparison was made between the results obtained in these two cases.

3. Numerical Derivations

The size and the refractive index of typical samples for the light of 550 mμ in wavelength were calculated. α, the characteristic of the particle, was obtained by interpolation from values of $(F+B)/B$ and $(F'+B)/(F+B)$ given in tables. For ZnO, three samples were used. Sample A and B had parallel beam in the transmitted light and sample C had not. Therefore, for samples A and B, $(F+B)/B$, and for sample C, $(F'+B)/(F+B)$ were used for calculation. For TiO_2 samples, $(F'+B)/(F+B)$ was used.

1) ZnO

Sample A (particle concentration 20% and thickness 15 μ)

With observed values $R=0.39$ and $T=0.52$, $(F+B)/B$ became 10.45 with which $\alpha=6.85$ and $B/E=8.4$ were found in tables and D became 0.81 μ. With this value of D, $N=1.45\times10^{11}$ was computed for a sample composed of clear lacquer 80 gr. (sp. gr.= 9.2) and ZnO powder 20 gr. (sp. gr.=5.5), and $E=40.2\times10^{-11}$ was derived.

Result: $D=0.81\ \mu$ and $n=1.89$ as seen in the accompanying figure in which values of E and α are plotted against $D(\mu)$ for $n=1.6$, 1.7,—, 2.7 at $n_0=1.5$ and $\lambda=$ 550 mμ according to relation (1). Left ordinate is for E and right ordinate for α.

Sample B (particle concentration 10% and thickness 20 μ)

With $R=0.275$ and $T=0.625$, D became 0.79 μ with which $N=0.75\times10^{11}$ was computed and $E=36.5\times10^{-11}$ was derived.

2) Hand Book of Chemistry and Physics, 40 th ed. (1958-59).

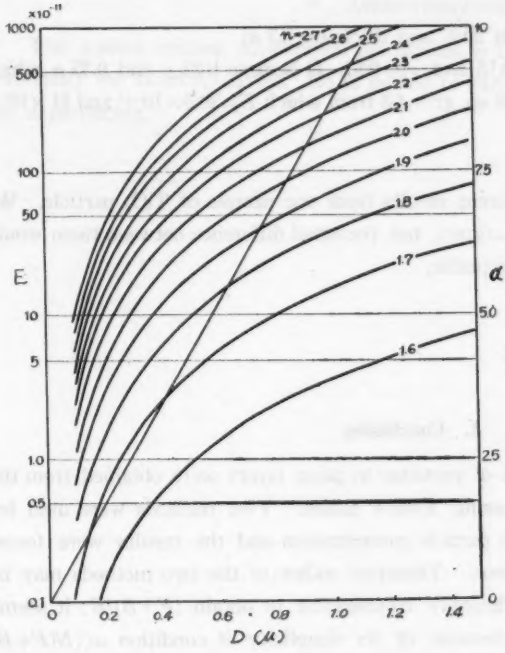

Values of E and α computed from $E=\pi D^3\tau_r/16$ and $\alpha=\pi Dn_0/\lambda$.

Result: $D=0.79\,\mu$ and $n=1.88$.

Sample C (particle concentration 20% and thickness 55 μ)

Constants r_0 and r_1 were determined from experimental conditions as 0.04 and 0.09 respectively. With observed values $r_2=0.46$, $\tau'=0.346$, $\tau=0.31$ and $T=0.24$, $(F'+B)/(F+B)=1.090$ was derived which gave $D=0.79\,\mu$ with which $N=1.5\times10^{11}$ and consequently $E=47.2\times10^{-11}$ were obtained.

Result: $D=0.79\,\mu$ and $n=1.91$.

From these results, the size of ZnO particle was found between 0.79 μ and 0.81 μ and the refractive index betwecn 1.88 and 1.91, which shows a good agreement between the results obtained by the two methods.

2). TiO_2

Anatase type (particle concentration 20% and thickness 50 μ)

With observed values $T=0.065$, $\tau'=0.126$, $\tau=0.11$ and $r_2=0.52$, $(F'+B)/(F+B)$ became 1.175 and α became in two values of 2 and 2.9 which gave two values for D: 0.23 μ and 0.33 μ. In consequence, we obtained two values 7.5×10^{12} and 2.8×10^{10} for N which, with sp. gr.=3.84, resulted in $E=27.4\times10^{-11}$ and 46×10^{-11}.

Result: $n=2.45$ and 2.4.

Rutile type (particle concentration 20% and thickness 13 μ)

With $T=0.17$, $\tau'=0.171$, $\tau=0.15$ and $r_2=0.51$, D became 0.22 μ and 0.35 μ which gave $N=7\times10^{12}$ and 1.8×10^{12} with sp. gr.=4.3 from which $E=39.8\times10^{-11}$ and 81×10^{-11} were derived.

Result: $n=2.6$ and 2.55.

Thus we obtained two different results from one sample of TiO_2 particle. We can not tell which of the two is correct, but the small difference between them would allow either one to be equally acceptable.

3). $PbCO_3$

Result: $D=0.9\,\mu$ and $n=1.8$.

4. Conclusion

The size and refractive index of particles in paint layers were obtained from the reflectance and transmittance by using Ryde's tables. Two methods were used for samples of different thickness and particle concentration and the results were found to agree within experimental error. Therefore either of the two methods may be used in practice. But it is technically troublesome to obtain $(F+B)/B$; it seems preferable to use $(F'+B)/(F+B)$ because of its simplicity if condition $\mu\ll N(F+B)$ can be previously confirmed.

The derived sizes are reasonable in comparison with the result of examination under microscope. But the refractive indices are slightly smaller than the data given in reference. This discrepancy may be ascribed to that the evaluated N, the particle number in unit volume, happened to be a little too large in every experiment, probably caused by (1) N varied in mixing and sieving of paints, (2) state of particles changed by being in layer of dried paint, and (3) form of particles was assumed to be spherical. Nevertheless, the deviation is considered passable as far as practice is concerned, and the method of obtaining the size and refractive index of particles constituting the layer of dried paint by observing the behavior of penetrated light within the layer as done in the present work is as effective as the customary way of measuring them directly on samples of particles. It must be emphasized that the behavior of light within the paint layer is directly related to the reflectivity of the layer surface, and the reflectivity of surface is afterall what we are really concerned about in practice. The above method will be available for studying the reflectivity of paint surface.

5. Acknowledgement

The author wishes to express his thanks to Dr. Y. Uchida, professor of Kyoto University for valuable advise. He is debted to Mr. T. Satsutani for assistance during the experiments.

Spectrophotometric Studies on Inorganic Crystals. Part I. Absorption Spectra of Crystalline Hexamminecobalt(III) Salts

Yukio KONDO

Department of Chemistry, Rikkyo University (St. Paul's Univ.), Ikebukuro, Tokyo

(Received July 10, 1961)

Abstract

A simple microscope attachment to a Beckman DU spectrophotometer of low magnification (~100×) with a reflecting objective has been devised and absorption spectra of nine crystalline hexamminecobalt(III) salts in the region 230~1000 mμ have been measured with this apparatus. Results show that the general feature of the ligand field bands is not much different from those in aqueous solutions; shifts of band maxima and changes in half-value widths are small. A slight dichroism observed in the chloride suggests a little distortion of hexamminecobalt(III) cation in crystals which have lower symmetries than the complex cation.

1. Introduction

In a previous investigation[1], ultraviolet absorption spectra of crystalline hexamminecobalt(III) salts were measured by photographic microspectroscopy. It was found that, in addition to weak absorption bands due to the complex cation (ligand field bands), the crystals had an intense absorption band, the position of which was in general much more bathochromic than that in aqueous solution.

It was concluded that the intense absorption band in the crystals was due to the transfer of an electron from every anion to the complex cation, and this conclusion was confirmed by calculations of relative positions of the absorption band by the energy cycle method, which showed good agreement between values calculated and observed.

As the previous measurement was a qualitative one, it was impossible to compare the ligand field bands in crystals with those in solutions. For the purpose of obtaining quantitative absorption spectra of solid samples of microscopic size, the author devised an instrumental setup with a reflecting objective and allowed the conversion

1) Y. Kondo: *Bull. Chem. Soc. Japan*, **28**, (1955) 497.

of an ordinary photoelectric spectrophotometer to a microspectrophotometer to be made in an inexpensive, quick, and convenient manner.

By the use of this apparatus, absorption spectra of nine crystalline hexammine-cobalt(III) salts were measured with special attention given to shifts of band maxima, change in half-value widths, and dichroism in crystals.

(1) Microspectrophotometry.—A simple microscope attachment to a Beckman DU spectrophotometer was devised. Fig. 1 is a schematic representation of the apparatus.

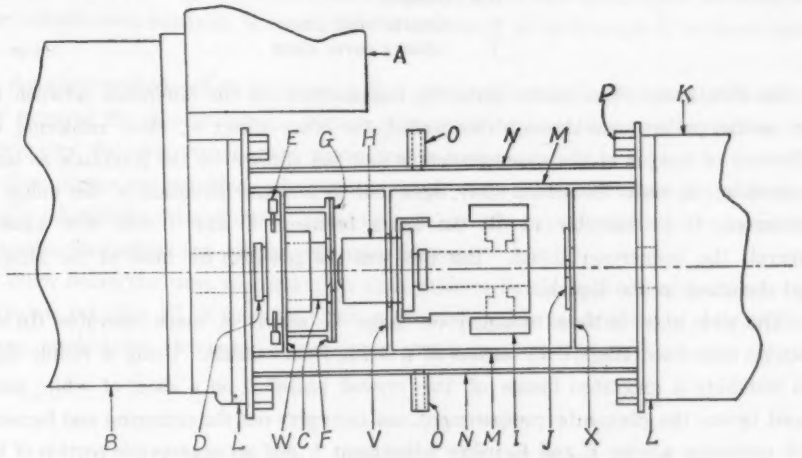

Fig. 1. Schematic representation of a microscope attachment to a Beckman DU spectrophotometer.

A	Light source housing	I	Focusing adjustment
B	Monochromator	J	Diaphragm
C	Reflecting condenser	K	Phototube compartment
D	Iris diaphragm	L	Bakelite plate
E	Centering screws	M, N	Side plate
F	Fixed stage	O	Water inlet and outlet
G	Movable stage	P	Screw
H	Reflecting objective		

In micro-use, the attachment is held by screws P on to monochromator B and phototube compartment K of the spectrophotometer. The microscope attachment is provided with reflecting condenser C and reflecting objective H which were used in the previous work[1]. The reflecting objective has the following specification: magnification 100×; numerical aperture 0.42~1.00; working distance 1.0 mm. The condenser is of the same specification as the objective except that the former has some aberrations.

Crystal Q and quartz plate Q′ (see Fig. 2), both being nearly equal in thickness, are laid on quartz slide glass S. They are closely placed and fixed with paraffin R

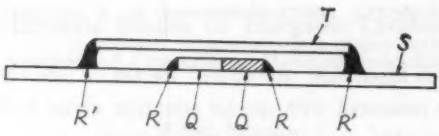

Fig. 2. Mounting of a crystal.

Q	Crystal
Q'	Reference quartz plate
R,R'	Paraffin
S	Quartz slide glass
T	Quartz cover glass

to the slide glass. The quartz plate, Q', compensates for the difference between the two optical paths — one through the crystal, the other direct —, thus rendering the difference of images of the monochromator exit slit thrown on the phototube as small as possible. In order to reduce stray light and to increase definition of the image by microscope, it is desirable to fill the space between T and T with 90% aqueous glycerol, the immersion liquid. But this was not possible, for most of the samples used dissolved in the liquid.

The slide glass is then mounted on stage G which is made movable 0.6 mm sidewise over fixed stage F by means of a string from outside. Using a visible light and watching a magnified image of the crystal projected on a sheet of white paper placed before the phototube compartment, one can carry out the centering and focusing with centering screws E and focusing adjustment I, and an appropriate portion of the image is selected by diaphragm J which limits the field to a rectangle. Readjustment is unnecessary in other ranges of the spectrum, for the reflecting objective is apochromatic.

Sensitivity of the phototubes is increased five times by substituting a 10,000 megohm resistor for the usual 2,000 megohm phototube load resistor. The increase in sensitivity nearly compensates for the loss of radiant energy through the microscope, so the ordinary hydrogen discharge tube is sufficiently bright to be used in the measurement down to 230 mμ. Plate V serves to cut off stray light, so do other two plates W and X, which support the condenser and diaphragm, respectively.

Polarized absorption spectra of crystals are measured with a polyvinylalcohol-iodine polarizer,[2] which is inserted between the monochromator and the microscope attachment. The polarizer is made rotatable about the optical axis of tha microscope. The apparatus can also be used for the measurement of absorption spectra at various temperatures. For this purpose, the space between side plates M and N is filled with

2) This was kindly provided by Dr. Y. Tanizaki of Tokyo Institute of Technology, to whom the author wishes to express his sincere thanks.

water at a given temperature through O. In this work, however, measurements were made at room temperature, about 20°C, without the use of water. Plate L on either side of the attachment is of bakelite for thermal insulation.

(2) Measurement of thickness of crystals.—Attempts were made to obtain correct thickness of the crystal.

The method, in which a piece of thin crystal is mounted, faces upright, on a paraffin-surfaced slide-glass and its thickness is measured with an eyepiece micrometer, gave considerable amounts of error, for the mounting at such angle is in most cases not easy.

Another method, which is usual in that a microscope is focused on the front and rear faces of the crystal and the difference between the focal distances is read on the micrometer dial, was found short of required accuracy.

One more method that was contemplated was the interference color method usually adopted for thin crystals. This method was of no avail, for hexamminecobalt-(III) salts themselves are colored yellowish brown.

Such being the case, discussion on intensities of ligand field bands in crystals had to be left for Part III of this series of work, in which application of interference fringe method by two-beam interference to hexamminecobalt(III) chloride crystals

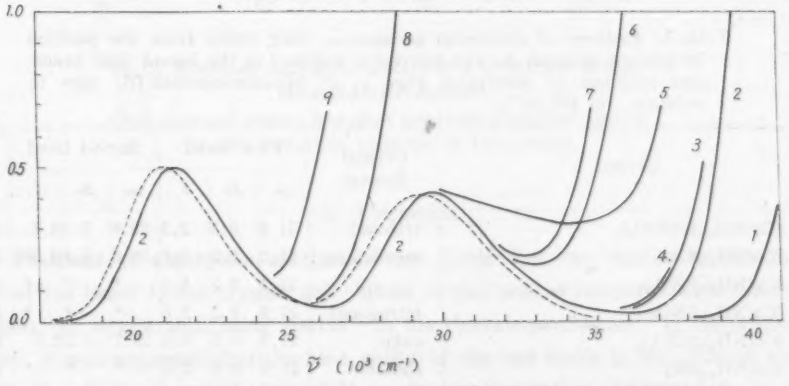

Fig. 3. Absorption spectra of hexamminecobalt(III) salts in crystals (full lines) and in solution (broken line).

In this figure, concerning the ligand field bands in crystals, only the first and the second bands of the chloride perchlorate, shifts of band maxima of which are the largest among the crystals studied, are shown.

1 $[Co(NH_3)_6](ClO_4)_3$
2 $[Co(NH_3)_6]Cl(ClO_4)_2$
3 $[Co(NH_3)_6]Cl\cdot SO_4\cdot 3H_2O$
4 $[Co(NH_3)_6]_2(SO_4)_3\cdot 5H_2O$
5 $[Co(NH_3)_6](NO_3)_3$
6 $[Co(NH_3)_6]_2(C_2O_4)_3\cdot 4H_2O$
7 $[Co(NH_3)_6]Cl_3$
8 $[Co(NH_3)_6]Br_3$
9 $[Co(NH_3)_6](NO_2)_3$

will be given. The interference fringe methods by two-beam and multiple-beam interferences will be explained in Part II.

In Fig. 3, which shows absorption spectra of hexamminecobalt(III) salts in crystals and in solution, absorption curves are conveniently so arranged that the intensities of maxima of the first bands in all crystals coincide with one another.

(3) Samples.—Samples were prepared according to the methods described in the papers cited in the previous report. As was stated in the previous report, stray light entering the objective from the exterior of the sample may produce a large error; this phenomenon is called Schwarzschid-Villiger (S-V) effect.[3] In order to reduce the stray light, crystals that had areas larger than the image of exit slit of the monochromator were used throughout this work. For assuring that the instrument and the crystals are free from defects, Lambert's law test should have been carried out on crystals of different thicknesses. But thin crystals of surface area large enough for this apparatus of low magnification were hard to obtain, so Lambert's law test was postponed until after the interference fringe method (see Part II) was established and another apparatus of higher magnification (see Part III) was devised, and hence in the present work, the aim was to include as many crystals of different anions as possible. Out of fourteen salts investigated in the previous work, nine salts shown in Table I were chosen as samples for the present work.

Table I. Positions of absorption maxima ν_m, their shifts from the position in aqueous solution $\Delta\nu$, and half-value widths l of the ligand field bands, and positions of absorption edge ν_e of hexamminecobalt(III) salts in crystals. (in $10^3\,cm^{-1}$).

Crystal	Crystal System	First Band			Second Band			ν_e
		ν_m	$\Delta\nu$	l	ν_m	$\Delta\nu$	l	
$[Co(NH_3)_6]Cl(ClO_4)_2$	trigonal	21.4	0.3	3.5	29.8	0.3	4.1	38.4
$[Co(NH_3)_6]Cl_3$	monoclinic	21.3	0.2	3.7	29.6	0.1	4.5**	34.4
$[Co(NH_3)_6](NO_2)_3$	...	21.3	0.2	3.6	...*	...*	...*	26.0
$[Co(NH_3)_6](NO_3)_3$	tetragonal	21.3	0.2	3.6	...*	...*	...*	36.4
$[Co(NH_3)_6](ClO_4)_3$	cubic	21.3	0.2	3.5	29.7	0.2	3.9	40.6
$[Co(NH_3)_6]Br_3$	rhombic	21.3	0.2	3.6	...*	...*	...*	27.9
$[Co(NH_3)_6]Cl\cdot SO_4\cdot 3H_2O$	rhombic	21.2	0.1	3.6	29.5	0.0	4.1	38.3
$[Co(NH_3)_6](C_2O_4)_3\cdot 4H_2O$	...	21.2	0.1	3.6	29.5	0.0	4.3**	34.9
$[Co(NH_3)_6]_2(SO_4)_3\cdot 5H_2O$	monoclinic	21.1	0.0	3.6	29.4	−0.1	4.1	38.3
Aqueous solution (Perchlorate)		21.1	0.0	3.5	29.5	0.0	4.1	

...* Covered by another band.
** Uncertain because of being covered partly by another band.

3) See for example: H. Naora: *Science*, **114**, (1951) 279; **115**, (1952) 248; *Biochim. Biophys. Acta*, **9**, (1952) 582.

2. Results

Results obtained by natural light are summarized in Fig. 3 and Table I. As is seen from Fig. 3, it is apparent that the general feature of two ligand field bands in the crystals is not much different from that in aqueous solution in contrast with the remarkable red shift of absorption edge in the crystals, which was discussed in the previous paper. The positions[4] of the absorption edge are also given in Table I. Results obtained by polarized light on a chloride crystal are given in Fig. 4.

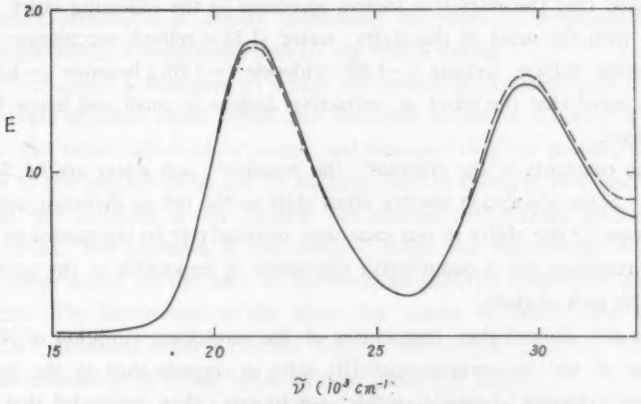

Fig. 4. Polarized absorption spectra of a crystalline hexamminecobalt(III) chloride.
(Full line and broken line show polarized absorption spectra at two extinction positions of the crystal).

3. Discussion

(1) Positions of absorption maxima.—From Table I it can readily be seen that most of the bands in the crystals are shifted to the blue as compared with those in solution, the largest shift being 300 cm^{-1} in the chloride perchlorate. In the previous paper[1], it was suggested that the blue shifts of the two bands in the crystals were due to the effects of crystal lattice field on the complex cation. Larger shifts in the chloride and the chloride perchlorate may be due to this effect, for the chloride anion has a larger ionic potential than those of the other anions. Smaller shifts in the chloride sulfate, the oxalate, and the sulfate might be interpreted in a similar way, for these salts have water of crystallization, which can be expected to act as a diluent

4) These were conveniently defined as the wavelengths of the point in an edge absorption curve that has the same intensity as that of the maximum of the second ligand field band.

and so reduce electrostatic fields of anions.

However, we must take into account other effects which influence the bands, for in crystals, refractive indices, dielectric constants, and specific interactions such as hydrogen bonding between the complex cations and anions, which are the principal factors of solvent effects[5], differ from those in aqueous solution. In the following several paragraphs, we shall discuss briefly the effects of these factors on the absorption bands observed in our work.

A preliminary test on refractive indices (n_D) of these crystals by the immersion method showed that the refractive indices increased in the following order, which is inconsistent with the order of the shifts: water (1.33)<sulfate, perchlorate (~1.56)< nitrate, chloride sulfate, oxalate (~1.60)<chloride (~1.70)<bromide (~1.76). It is generally accepted that the effect of refractive indices is small and hence is masked by other effects.

Dielectric constants of the chloride[6], the bromide[6], and water are 7.6, 7.5, and 81, respectively. Since absorption spectra often shift to the red as dielectric constants of solvent increase,[5,7] the shifts in our case may qualitatively be interpreted as the effect of dielectric constant, but a quantitative discussion is impossible at the present stage because of the lack of data.

Fujita et al.[8] showed that frequencies of the stretching vibration of N-H bonds in ammonias of the hexamminecobalt(III) salts in crystals shift to the red in the order: fluoride>chloride>bromide>iodide>perchlorate; they concluded that the shift is due to hydrogen bondings between the nitrogen atoms and anions, and that the hydrogen bond in the fluoride is the strongest and in the perchlorate negligibly small. In our case, especially in the chloride, there are other evidences that favor the existence of the hydrogen bond, the solvent cage effect and the dichroism, which will be mentioned in the following paragraph and in section (3), respectively.

Bayliss and Rees[9] interpreted the blue shift of a bromine band observed in liquid bromine from the position of the same band observed in gaseous bromine as follows: in the liquid the solvent cage compresses the Morse potential curve in such a way that the unsymmetrical shape of the curve becomes symmetrical, and consequently the equilibrium position of one atom approaches to that of the other atom, thus there is a transition from the ground state requiring more energy, a transition that leads

5) See, for example: Y. Ooshika: *J. Phys. Soc. Japan*, **9**, (1954) 594.
6) K. Nakano and A. Satsuka: Abstract of the Symposium on Coordination compounds on Sept. 22, 1960.
7) K. Ito and Y. Kuroda: *J. Chem. Soc. Japan, Pure Chemistry Section*, **76**, (1955) 934.
8) J. Fujita, K. Nakamoto, and M. Kobayashi: *J. Am. Chem. Soc.* **78**, (1956) 3295.
9) N. S. Bayliss and A. L. G. Rees: *J. Chem. Phys.*, **8**, (1940) 377.

to a blue shift. The solvent cage may also change the Morse potential of excited state, thus influencing the position of the band as well as changing the shape of the band. In crystals, it is natural to assume such a cage, because a crystal lattice is the extreme of a solvent cage and in the formation of the solvent cage hydrogen bonds must play an important role.

In the previous work[1], it was concluded that strong absorptions found in crystals were due to the transfer of an electron from every anion to the complex cation. If this is correct, this transition would affect the transitions within the complex cation. In this respect, structures of doubly protonated dicyanobis(1,10-phenanthroline)-iron-(II) and dicyanobis(2, 2′-bipyridine)-iron(II) are worth noting.

Schilt[10] proposed a structure in which one proton is symmetrically situated with respect to three adjacent donor atoms and the other proton is similarly disposed with respect to the other three donor atoms, and assumed that the protons are attracted and bound to the central metal ion by electron pairs in normally non-bonding orbitals. In some of our crystals, if we replace the protons with anions, similar structures would be found. For example, in the iodide[11], there are two kinds of iodide ions, one being those found on the tops of hexamminecobalt(III) octahedron and the other on the faces. The iodide ions on the faces are nearer to cobalt than those on the tops, the Co–I distances being 4.7 Å and 5.45 Å, respectively, therefore the former is expected to interact with cobalt more strongly than the latter.

Thus we must take into consideration varied effects, some of which will shift the bands to the blue and some to the red, and at the present stage, it is not possible to conclude which of the effects mentioned above plays the most important role in the crystals.

Frome Table I it can also be seen that in the chloride, the chloride sulfate, and the oxalate, the shift is larger in the first band than in the second one. The difference in behavior of the two bands is also demonstrated in the substitution of a ligand or ligands[12], effect of temperature[13], and effect of solvent[14], in which the same tendency, — the shift is larger in the first band than in the second — is observed. As for the effect of temperature and of solvent, the difference in behavior of the two bands has not been discussed theoretically but the substitution was given a theoretical explanation on the basis of quantum mechanics. It was shown[15] that each band splits

10) A. A. Schilt: *J. Am. Chem. Soc.*, **82**, (1960) 5779.
11) K. Meisel and W. Tiedje: *Z. anorg. Chem.*, **164**, (1927) 223.
12) See, for example: K. Sone: *J. Chem. Soc. Japan, Pure Chemistry Section*, **71**, (1950) 270.
13) Y. Kondo and M. Nakahara: *J. Spectroscopical Soc. Japan*, **7**, (1954) 17.
14) K. Nakamoto, M. Kobayashi, and R. Tsuchida: *J. Chem. Phys.*, **22**, (1954) 957.
15) H. Yamatera: *Bull. Chem. Soc. Japan*, **31**, (1958) 95.

into two sub-bands in unsymmetrical ligand fields and that the separation of the sub-bands is larger in the first bands than in the second. We can interpret the difference in the crystal spectra in the same way as in the substitution, because unsymmetrical crystal lattice fields correspond to unsymmetrical ligand fields. The similarity in shift of the two bands found in the perchlorate supports this view, for the perchlorate crystal and the complex cation are of the same cubic symmetry.

(2) **Half-value widths.**—As was stated in the previous report, the larger the extinction value is, the larger the S-V effect becomes. This makes absorption intensities near the maximum smaller than their actual values, and, in consequence, the shape of the absorption band becomes flatter and therefore the half-value width becomes broader than their respective actual ones.

Since Lambert's law was not tested in the present work, the present results can not be assured not to include S-V effect. However, it is apparent from Table I at least that the half-value widths are nearly the same as those in solution. This confirms the previous statement that Kobayashi's data[16] on similar crystals are affected much by stray light, for absorption bands obtained by him are remarkably flattened.

Here also we must take into consideration the other effect, the solvent cage effect mentioned above, which affects the half-value width, because this effect reduces the amplitude of vibration in the ground state making the half-value width smaller. Bayliss attributed to this effect the smallness of half-value width of bromine in chloroform in comparison with that in gas. Smallness of value observed in the second band of the perchlorate when compared with that in solution may be interpreted by this effect, for in this crystal we need not take into account the splitting which is due to the crystal field having a symmetry different from that of the complex cation.

(3) **Dichroism.**—In order to observe some other effect of crystal fields on the two bands, polarized absorption spectra, were measured on several crystals, but only the chloride and a double chloride with zinc chloride, $[Co(NH_3)_6]Cl_3 \cdot ZnCl_2 \cdot H_2O$, showed weak dichroism. The result obtained on the chloride is shown in Fig. 4.

It is seen from this figure that the signs of dichroism of the two bands are reversed. Since crystals having crossed dispersion curves are rare, this reversal reduces the possibility that it is due to a difference between refractive indices in two crystalline directions,[17] and leads to a conclusion that the dichroism observed is the real dichroism of the complex cation. Moreover, the fact that complex cations with

16) R. Tsuchida and M. Kobayashi: "The Colors and Structures of Metallic Compounds" (in Japanese), Zoshindo, Osaka, 1944, p. 180.

17) Optical path lengths within a crystal depend upon the numerical aperture of the reflecting objective and the refractive index of the crystal (see Part III of this series of papers).

symmetries lower than the symmetry of the hexamminecobalt(III) ion show in crystals a similar but strong dichroism[16,18] confirms the above conclusion. Typical examples of the dichroism observed with the present apparatus are given in Fig. 5.

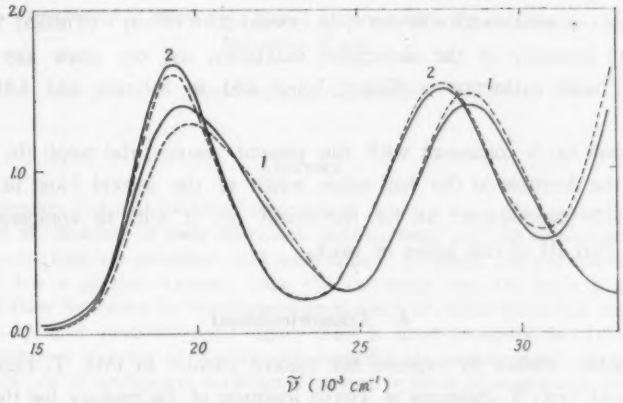

Fig. 5. Polarized absorption spectra of a pentammine- and a tetramminecobalt(III) salt in crystals.
(Full lines and broken lines show polarized absorption spectra at two extinction positions of the crystals).
1. $[Co(NH_3)_5H_2O](SO_4)_3 \cdot 3H_2O$ 2. $[Co(NH_3)_4CO_3]NO_3 \cdot 0.5H_2O$

There are two causes which produce dichroism in symmetrical hexamminecobalt-(III) cation. They are the indirect effect of an unsymmetrical crystal field and the direct effect of ligands that were distorted by an unsymmetrical arrangement of ions. At present, it is not possible to discuss this subject in detail, for crystal structures of hexamminecobalt(III) salts, except those with a cubic symmetry, are not known. However, the fact that the hydrogen bonding is the strongest in the chloride as mentioned above and that crystals, with unsymmetrical crystal structures except chloride crystal, do not show dichroism seem to favor the direct effect of ligands; this inference is consistent with the conclusion given by Van Vleck[19] to interpret the magnetic behavior of vanadium, titanium, and chromium alum.

(4) Comparison of the present results with others.—Among the few studies on quantitative measurements of absorption spectra in crystals of the first transition

18) S. Yamada and R. Tsuchida: *Bull. Chem. Soc. Japan*, **33**, (1960) 98.
19) J. H. Van Vleck: *J. Chem. Phys.*, **7**, (1939) 61.

metal complexes,[20] works reported by Tréhin [21] and by Vuldy[22] deserve mention. Using a large single crystal of nickel(II) sulfate heptahydrate, they obtained the following results for the near ultraviolet absorption band, the maximum of which in aqueous solution lies at $25.3\times10^3\,cm^{-1}$. (a) The position of the absorption maximum shifted to the blue by $400\,cm^{-1}$ in the crystal. (b) The half-value width[23] decreased in the crystal: in solution $2.9\times10^3\,cm^{-1}$, in crystal $2.5\times10^3\,cm^{-1}$ (Tréhin) $2.7\times10^3\,cm^{-1}$ (Vuldy). (c) Intensity of the absorption maximum did not show any appreciable change, the molar extinction coefficient being 4.81 in solution and 4.84 in crystal (Vuldy).[24]

The result (a) is consistent with the present results; the result (b) would seem to support the decrease in the half-value width of the second band in the hexamminecobalt(III) perchlorate; as for the result (c), it will be compared with the author's in Part III of this series of work.

4. Acknowledgment

The author wishes to express his sincere thanks to Prof. T. Uemura of this laboratory and Prof. Y. Inamura of Tokyo Institute of Technology for their valuable advice and encouragement throughout this work. Much appreciation is also due to the members of the Laboratory of Inorganic Chemistry, Tokyo Institute of Technology, where a part of the present work was done, for their valuable advice and discussion.

20) Although Tsuchida and Yamada made many measurements about this subject and obtained interesting results, it seems to the author that their data are affected much by stray light and are therefore only qualitatively significant. For example, in spite of their statement that the S–V effect is very small, their data on trisethylenediaminecobalt(III) salts (see ref. 18) show that half-value widths increase from $3.5\times10^3\,cm^{-1}$ in solution to $4.0\times10^3\,cm^{-1}$ in crystals. These results can only be justified if we attach importance to the S–V effect in view of what we have learnt about the half-value width. In Part III of this series of work a more detailed discussion about the relation between the S–V effect and half-value widths will be given.

21) R. Tréhin: *Compt. rend.*, **216**, 558 (1943).

22) G. Vuldy: *ibid.*, **228**, 1414 (1949).

23) Calculated by the present author from their data.

24) An anomalously lower value obtained by Tréhin for the crystal was attributed by Vuldy to an experimental error.

Spectrophotometric Studies on Inorganic Crystals. Part II. Measurement of Thickness of Thin Crystals by Interferometry

Yukio KONDO

Department of Chemistry, Rikkyo University (St. Paul's Univ.), Ikebukuro, Tokyo

(Received July 25, 1961)

Abstract

Two-beam and multiple-beam interference methods are applied to the measurement of thickness of some inorganic monocrystals and the advantages of the two methods are compared with each other. Although the multiple-beam method has a greater accuracy than the two-beam one, the latter is more suitable than the former for microspectrophotometry of rather thick and colored crystals. Use of monochromatic lights from a monochromator is advisable, for continuous varying of wavelength simplifies the measurement. In some instances, use of continuous variation of refractive index of medium is advantageous. The relation between interference fringes by monochromatic-light and white-light is experimentally investigated.

1. Introduction

For quantitative measurement on light absorption of monocrystals, it often becomes necessary to use micron-sized crystals. In such cases of spectrophotometry, use of a microscope is desirable, and in the previous studies[1,2] applications of microscope techniques to the measurement of absorption spectra of crystalline hexamminecobalt(III) salts were given. Use of interferometrical techniques is also indispensable for accurate measurement of the thickness of thin crystals at the cross-section used for absorption measurement.

Bree and Lyons[3] made a comparison between two interferometrical methods, which we call here the interference band method and the interference fringe method[4],

1) Y. Kondo: *Bull. Chem. Soc. Japan*, **28**, (1955) 497.

2) Y. Kondo: This Journal, **10**, (1961) 7.

3) A. Bree and L. E. Lyons: *J. Chem. Soc.*, **1956**, 2658.

4) In the paper of Bree and Lyons, the two methods were called the two-beam method and the multiple-beam method. In this paper the terms, two-beam method and multiple-beam method, are used to mean "two-beam interference fringe method and multiple-beam interference fringe method."

and stated that the former was slightly better than the latter. In the interference band method[5], absorption bands, due to the interference arising from light being reflected from both the front and the rear surface of a crystal, are measured with a spectrophotometer, and the wavelengths of maxima and minima of the absorption combined with the refractive indices of the crystal at those wavelengths give the thickness.

Interference absorption bands are usually very weak, so the application of the interference band method to inorganic crystals is possible only in cases of colorless crystals. On the other hand, the interference fringe method, in which displacements of interference fringes due to a crystal are measured at several wavelengths, can be applied to colored crystals if we choose proper wavelengths. In the present work, interference fringe methods, in which both the two-beam and the multiple-beam interferences are included, are re-examined with a microinterferometer, and the use of continuous variation of wavelength and refractive index of medium is studied,

2. Apparatus

A Twyman-Green type microinterferometer was used.[6] The apparatus, shown schematically in Fig. 1, is of a Michelson type which enables the two-beam interference to be observed. Modification of the apparatus from the Michelson type to a Tolansky one is made readily by removing Q_1, Q_2, and M_2 in Fig. 1 and covering the crystal placed on mirror M_1 with a semi-metallized slide glass so as to make a wedge of air between the slide glass and the mirror.

3. Comparison between two-beam interference method and multiple-beam interference method

Remarkable sharpening of interference fringes by multiple-beam interference in contrast with two-beam one is well known and was clearly observed in this study. The superiority of multiple-beam interference method over two-beam interference method in accuracy of thickness measurement is thus obvious. But, there are the following several difficulties when we apply the multiple-beam method to microspectrophotometry.

(a) Use of a rather pure monochromatic light as the light source is necessary

5) This method is a refinement of the method by visual observation of interference color, as was stated by Bree and Lyons.

6) Made by Olympus Optical Co., Ltd. Tokyo.

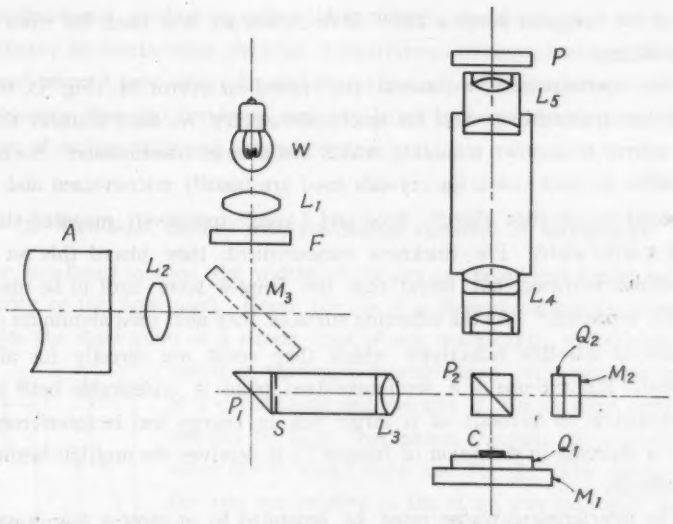

Fig. 1. Schematic representation of the microinterferometer used.

A	Monochromator	M_1, M_2, M_3	Plane mirror
C	Crystal	P	Polarizer
F	Filter	P_1	Totally reflecting prism
L_1, L_2	Condensing lens	P_2	Biprism
L_3	Collimating lens	Q_1, Q_2	Quartz slide glass
L_4	Objective 6×, 12×	S	Pinhole
L_5	*Eyepiece*	W	Tungsten lamp

for producing multiple-beam interference.[7] Available wevelengths are thus limited to a few, emitted by a sodium lamp and a mercury vapor lamp: 5890–5896 (Na): 5770–5790, 5461, and 4360 Å (Hg). This makes it impossible to apply the multiple-beam method to colored crystals that absorb some of the lights mentioned above. An attempt was made to use a monochromatic light from a monochromator with a tungsten filament lamp as the light source. For this purpose, the single monochromator of a Hitachi EPU-2 quartz photoelectric spectrophotometer and a 10 V 5 A tungsten lamp with voltage higher than nominal were used. To produce the multiple-beam interference fringes, the slit width was found necessary to be reduced to 0.01~0.02 mm at 600 mμ which was equivalent to about 0.5 mμ effective band width. But, with these slit widths, the image on the microscope was too dim for succesful observation.

7) S. Tolansky, "Multiple-Beam Interferometry of Surfaces and Films", Oxford Univ. Press, London (1948), p. 21. The experimental condition (3) for the production of highly sharpened multiple-beam Fizeau fringes: monochromatic light, or at most a few widely-spaced monochromatic wavelengths, should be used.

In place of the tungsten lamp, a 220 V 10 A carbon arc was used, but even this was found insufficient.

(b) For interferometry, we mount the crystal on mirror M_1 (Fig. 1), which has practically no transmission, and for spectrophotometry, we need transfer the crystal from the mirror to another mounting which has a large transmission. Such transfer is not possible in most cases, for crystals used are usually micron-sized and, in some cases, adhered to the slide glass.[8] Bree and Lyons[9] tentatively mounted the crystal on a clear quartz plate. For thickness measurement, they placed this set between two metallized surfaces, but found that the fringes were hard to be observed as theoretically predicted.[9] As the reflecting surfaces, they next used aluminum deposited quartz plates of 30~40% reflectivity which they could use directly for absorption measurement. But the use of a semi-metallized plate is undesirable both in micro-spectrophotometry on account of a large loss in energy and in interferometry on account of a decrease in definition of fringes[10]; it deprives the multiple-beam method of its advantage.

(c) The interfering surfaces must be separated by at most a few wavelengths of light, as is required by theory[9]. This makes it impossible to apply the multiple-beam method not only to thick crystals but also to thin crystals because, when they are grown on a piece of slide glass from solution and are left adhered on the glass, it is usual that they are accompanied with thicker crystals[8].

In the two-beam method with a Michelson type interferometer, two reflecting surfaces M_1 and M_2 (Fig. 1) are widely separated, therefore additional quartz slide glass Q_1 with the crystal mounted on it can be used and the change in optical path length caused by this quartz glass can be made up with another quartz glass Q_2 of the same thickness laid on M_2 which makes the fringes to be observed without much loss of definition. Thus the difficulties (b) and (c) in the multiple-beam method are not involved in the two-beam method and so is also the difficulty (1), for the use of monochromatic light from a monochromator is possible in the two-beam method as will be seen in the next section.

As is well known, the percentage error in measuring the thickness by interferometry becomes small with the increase of crystal thickness. Therefore, if we

8) For the production of flat crystals suitable for absorption measurement, it is recommended, if possible, to evaporate a solution directly on a slide glass. Then the crystals grown are adhered to the slide glass. See Part III of this series of papers.

9) S. Tolansky, ibid. p. 21. The experimental condition (4): the interfering surfaces must be separated by at most a few wavelengths of light.

10) S. Tolansky, ibid., p. 21. The experimental condition (1): the surfaces must be coated with a highly reflecting film of minimal absorption.

apply the two-beam method to rather thick crystals, the weak point of the method, the uncertainty in determining the shift of interference fringes, becomes unimportant.

In conclusion, it may safely be said that although the multiple-beam method has greater accuracy than the two-beam one, the latter is more suitable to microspectrophotometry of rather thick and colored crystals.

3. Two-beam method with continuous variation of wavelength

In the two-beam method, the widths of fringes are broad and almost independent of the purity of the light used. Hence, the use of a monochromator becomes possible and enables the application of a strong light of any wavelength, simplifying the procedure of thickness determination. Observations were made at a crystal edge and two sets of fringes were compared, the one due to light that passes through the crystal and the other due to direct light (see Fig. 2). The displacement of the one set relative to the other was expressed in units of fringe separation, but only the fractional part, f, of the total, $n+f$ (n integral), was observable since monochromatic lights are used with which the zero order fringes became indiscernible.

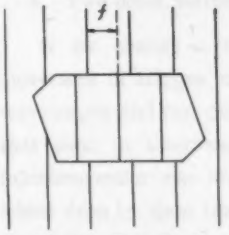

Fig. 2. The displacement of interference fringes by a crystal.

In Bree and Lyon's original work, observation were made at several wavelengths by the use of a sodium lamp and a mercury vapor lamp, and from the group of f values so obtained for various values of λ, d was determined graphically [d is the physical thickness of the crystal]. For given λ, μ_o and μ, [μ_o is the appropriate refractive index of the crystal, μ the refractive index of the surrounding medium], plot of d [$d=(n+f)\lambda/2(\mu_o-\mu)$] against $(n+f)$ is linear, so for a given crystal a chart may be drawn similar to that shown in Fig. 3 which is for a potassium chloride crystal. On this chart, the value of d which correlates best with the observed group of f values can be found.

In the present work, observation was made with the light from a monochromator. At a given wavelength λ, f was read, then by turning the wavelength dial of the monochromator, the movement of interference fringe was followed, and at another wavelength λ', f' was read. Since the fringe was being shifted continuously, we could determine the difference $\Delta(n+f)$ of fringes between λ and λ'. The intersecting point of the straight line for λ' in Fig. 3 with a straight line that is parallel to and by $\Delta(n+f)$ apart from the line for λ directly indicates the thickness of the crystal.

The advantages of the use of continuous variation of wavelength are as follows. (a) Although, of course, the more the better, two wavelengths and hence two re-

fractive indices of the crystal suffice. This is important, as the measurement of refractive indices of crystals is usually considerably difficult. (b) Direction of the fringe displacement, right or left, becomes obvious, which can not immediately be determined when we use discontinuous light source. (c) Since suitable wavelengths can be chosen at will, we can avoid the wavelength at which the crystal absorbs light.

Probably, the only weak point of the use of a monochromator is that the monochromatic light is not pure, it obviously causes error on λ and moreover may

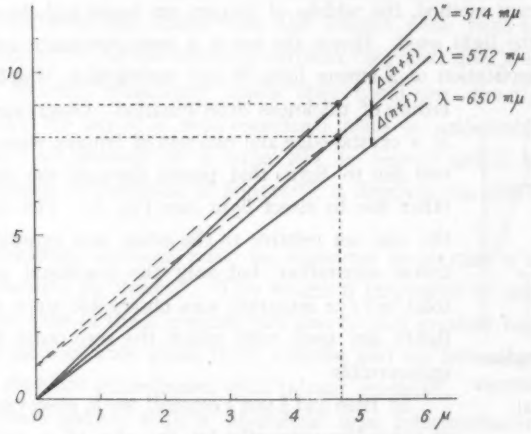

Fig. 3. Relation between fringe displacement and crystal thickness in potassium chloride.

Table I. Values of λ, μ_e, $n+f$, $\Delta(n+f)$, and d for two potassium chloride crystals.

Crystal 1.

λ*	μ_e	$n+f$	$\Delta(n+f)$	d*	
0.514	1.496	9	1	4.660	Mean
0.572	1.491	8	1	4.660	$d=4.661\pm0.002\ \mu$
0.650	1.488	7		4.663	

Crystal 2.

λ*	μ_e	$n+f$	$\Delta(n+f)$	d*	
0.510	1.496	70	4	35.90	Mean
0.538	1.494	66	4	35.86	$d=35.86\pm0.04\ \mu$
0.569	1.491	62		35.83	

* In microns.

increase error on f if this impure monochromatic light reduces the definition of fringes. But, in the present experiment, effective band widths were within 2 mμ throughout the visible region. Errors on λ are thus comparable to or sometimes much smaller than the error on $(n+f)$, which is considered to be about 0.1. Changing of the light source from the monochromator to a sodium or a mercury vapor lamp did not affect the definition of fringes, so errors due to the use of monochromator are of no account in the two-beam method. For minimizing the error on f, if the crystal is rather thick, it is recommended to choose the wavelengths at which two sets of fringes coincide at the crystal edge; such wavelengths for two potassium chloride crystals are given in Fig. 3 and Table I.

4. Two-beam method with continuous variation of refractive index of medium

If we change a refractive index of medium continuously, we can follow the movement of fringes in the same manner as in the case of continuous variation of wavelength and can determine $\Delta(n+f)$. This is an experimental technique similar to that used in interference refractometers. To carry out this, the lower part of the interferomenter was immersed in ethyl alcohol (μ=1.364), and aniline (μ=1.586) was added drop by drop from a burette while stirring and part of the mixed solution was pipetted out at times. After about 40 ml of aniline was added to 100 ml of ethyl alcohol, the refractive index of the medium became 1.438 and the movement of the fringe was 1.0. A treatment similar to the one described in section 3 gave 4.1 μ as the thickness of a hexamminecobalt(III) bromide crystal.

Difficulties encountered in carrying out this method are as follows. To accomplish thorough mixing of the two liquids, (a) fairly violent stirring of the liquid mixture was necessary; it often caused the crystal to move. To avoid this, the crystal was fixed on to slide glass Q_1 with paraffin. (b) The procedure took a fairly long time, for example, about one hour in the above experiment. (c) In order to avoid the penetration of the liquid into the apparatus, especially the collimator and the biprism, shielding of these with paraffin was necessary.

The advantage of this method is that only one refractive index of the crystal suffices for measuring the thickness. Hence, the use of the method is advisable when the refractive index can not be measured but can be found elsewhere in tables or in literature (usually for D line) as is often the case.

5. Relation between monochromatic-light and white-light interference fringes

The apparatus used in the present work was originally designed for the inspection of surfaces of polished opaque materials, especially, metals. For such purposes, a

light source such as a tungsten lamp is used and a dark fringe seen between colored fringes indicates the zero order interference fringe between the mirror and the surface of the metal, displacement of the dark fringe of one surface relative to another one showing the distance between them. When a crystal is placed on the reflecting surface, the dark fringe which appears on the crystal no longer represents the zero order interference fringe, because optical paths within the crystal depend on wavelength, hence the displacement of the dark fringe on the crystal relative to the reflecting surface does not indicate the thickness of the crystal.

The relation between monochromatic-light and white-light interference fringes is given in text-books[11] Let n' be the displacement of the dark fringe measured in units of monochromatic light fringe of wavelength λ and n the real displacement of this monochromatic-light fringe, and assume that μ_c follows Cauchy's dispersion formula,

$$\mu_c = A + \frac{B}{\lambda^2}, \quad \cdots\cdots(1)$$

then, $n'-n$ is given by

$$n'-n = \frac{4Bd}{\lambda^3}. \quad \cdots\cdots(2)$$

B was calculated to be 0.0059 for potassium chloride from the values of refractive indices in the visible region. For the two crystals mentioned in Table I, $n'-n$ was calculated to be 0.82 at 514 mμ (crystal 1) and 6.5 at 510 mμ (crystal 2), while observed values were about 1.0 and 5.0 respectively.

If we use Hartmann's dispersion formula,

$$\mu_c = A + \frac{B}{\lambda_0 - \lambda}, \quad \cdots\cdots(3)$$

instead of Cauchy's one, we obtain

$$n'-n = \frac{2Bd}{(\lambda_0-\lambda)^2}. \quad \cdots\cdots(4)$$

B and λ_0 were calculated to be -0.0076 and $0.217\,\mu$, respectively, for potassium chloride; for the crystals mentioned above, $n'-n$ was calculated to be 0.76 at 514 mμ (crystal 1) and 6.3 at 510 mμ (crystal 2).[12]

For the crystals mentioned above the monochromatic-light fringe displacements were 9 at 514 mμ (crystal 1, see Table I) and 70 at 510 mμ (crystal 2), while the white-light fringe displacements were 10 and 75, respectively. Thus the white-light

11) See, for example: T. Hori, "Physical Optics" I. (In Japanese), Misuzu-Shobo, Tokyo (1952), p. 219.

12) Wavelength dependency of $n'-n$ was also examined, but the results showed that there is no depenpency, that is, that $n'-n$ has the same value for all wavelengths examined in spite of the fact that according to the formula (2) or (4), $n'-n$ is inversely proportional to λ^3 or $(\lambda_0-\lambda)^2$. The reason for this discrepancy between the theory and the experiment remains unexplained.

interference fringe can not be applied for accurate measurements of the thickness of crystals, nevertheless it is useful for preliminary test of crystals in microspectrophotometry as it affords quick information about the approximate thickness and uniformity of a crystal and makes it easy to select the sample suitable for absorption measurement.

6. Acknowledgment

The present author wishes to express his sincere thanks to Prof. T. Uemura and Dr. M. Nakahara of this laboratory for their valuable advice and encouragement throughout this work.

Study of the Fechner Color with a Cathode-ray Tube

Yukihiko HARAI

Technical Bureau, Kansai Telecasting Company, Kita-ku, Osaka, Japan.

Abstract

A new experimental method for studying the Fechner color is described. The color phenomenon caused by intermittent light stimuli which is known as of the Fechner color has not been studied in detail because it is being regarded as singular in the field of the theory on color-sensation.

The Fechner color is usually realized by the rotation of disks such as the Benham top, and the observation has been only qualitative. In the new method described in this paper, a television picture tube is utilized to produce the Fechner color by which means quantitative measurements become possible.

The experiment is described and the results obtained are shown. A conclusion is reached that the Fechner color is not singular but very important and basic in the study of color.

1. Introduction

In 1958, while undertaking research on color television, the author by chance noticed RP and P colors on a black and white television tube when vertical and horizontal synchronization broke down. This was witnessed by several others who were present; it seemed a fairly common phenomenon, not a mere illusion. Investigation on the nature of this phenomenon led the author to the present study of the Fechner color with a cathode ray tube. Subsequently, it was found that the phenomenon is none other than that found by Fechner in 1838 with a rotating disk shown in Fig. 1. The color perceived by such device has been called the Fechner color or the subjective color. Since Fechner's discovery, this subject has been taken up by many scientists, all of them using the rotating disk method which has so far failed to reveal the crux of the problem.

Among the rotating disks used for these experiments, the Benham top shown in Fig. 2 is most famous. This Benham top was devised by Benham in 1894; it consists of a disk, the half of which is painted black, and the other half has four groups of black lines painted on it. Each of these groups consists of three concentric arcs with the center angle of 45°.

This pattern produces most distinctive tints, hence in the study of the Fechner

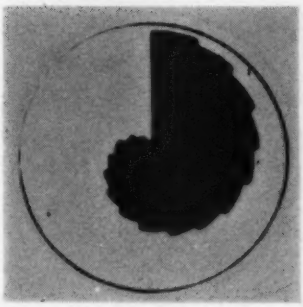

Fig. 1

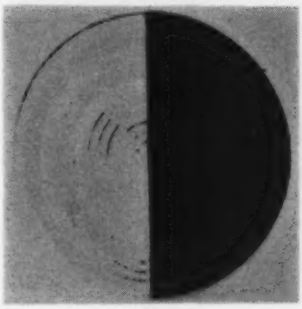

Fig. 2

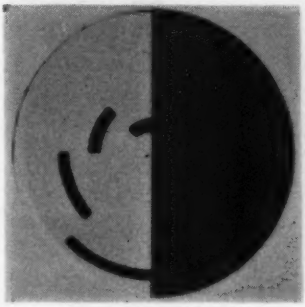

Fig. 3

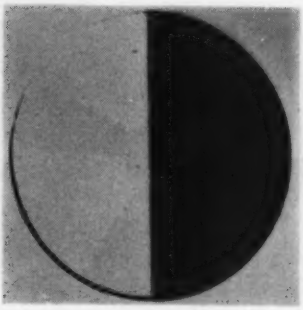

Fig. 4

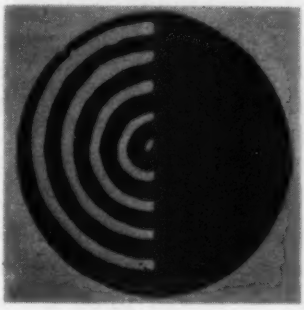

Fig. 5

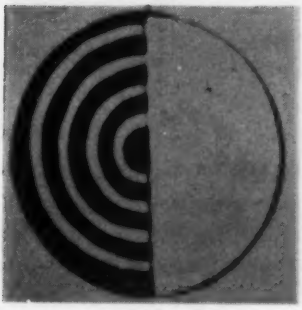

Fig. 6

color, the Benham top or its modifications are most widely used.

Benham and Lineing (1894) used sodium light instead of the sunlight to illuminate the disk, and Ahneg (1894) used monochromatic light sources and their mixtures.

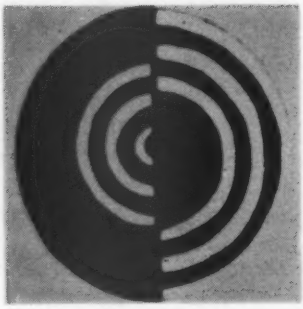

Fig. 7

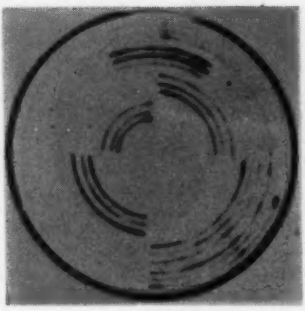

Fig. 8

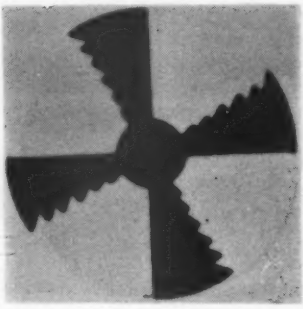

Fig. 9

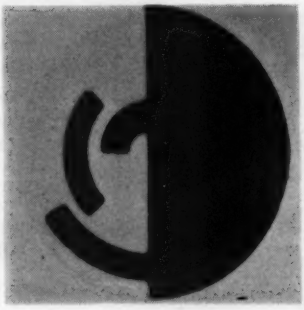

Fig. 10

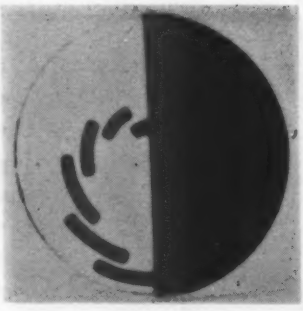

Fig. 11

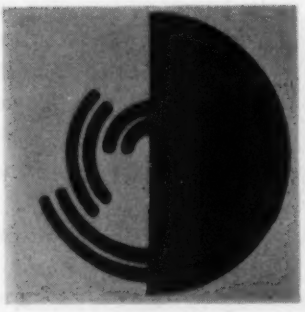

Fig. 12

Finnegan and Moore (1894) devised several kinds of disk shown in Figs. 5, 6 and 7. Bidwell (1897) devised a special rotating disk: the disk is divided into three equal sectors, one sector is cut off, one of the remaining sectors is blackened and the other whitened. He made some experiments with this disk changing the luminosity, rotating speed and the direction of the rotation.

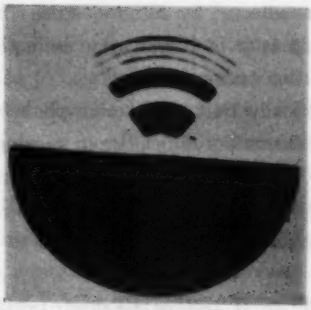

Fig. 13

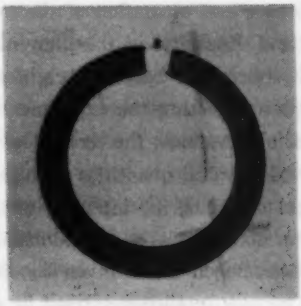

Fig. 14

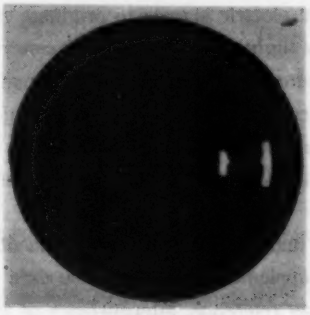

Fig. 15

Bagley (1902) used a disk shown in Fig. 8 for his study on relations among rotating speed, width and length of lines, relative dimension of sectors, intensity of illumination and background of the rotating disk.

Baumann (1912–1918) prepared disks shown in Figs. 9, 10, 11 and 12, and studied the effects of illumination, order and length of sectors, size of the disk and distance between the observer and the disk. Piéron (1922) made observations with a disk shown in Fig. 13 illuminated by monochromatic light. Fry (1933–1934) devised disks with apertures varying in size, shape and position as shown in Figs. 14 and 15. The disk was placed between the observer and a source of light, and the relations of frequency of the light stimulus and light intensity of every stimulus to the produced Fechner color were studied.

The results obtained by a number of studies referred above proves that the phenomenon of the Fechner color is real. To sum up their results: the Fechner color is observable only in a limited range of rotating speed of the disk; if the direction of rotation is reversed, sequence of the colors that appear is also reversed;

brightness and saturation of the Fechner color are affected by rotating speed of the disk and intensity of the illumination; as the intensity of illumination is increased, the Fechner color becomes brighter but its saturation becomes lower.

For conducting the experiment more systematically than those mere phenomenological observations, the method of rotating disk encounters difficalties in varying the involved physical quantities such as the frequency of light intermittence, the duration of light stimulus, the intensity of illumination, and so forth. Difficulties are also met with in obtaining good reproducibility of the experiment for many observers to view the phenomenon under given conditions.

The new method described in this article utilizes a picture tube of television receiver as the light source and the intermittence of iight is produced on the tube by the application of special electric signals to originate the Fechner color. By this method, duration of every light stimulus and frequency of intermittence are easily varied and accurately measured. Luminosity and contrast of the pattern can also be varied by adjusting the generating circuit. Such being the experimental setting, value of every physical quantity that is involved can be fixed enabling the Fechner color to become reproducible and many observers to judge the color appeared under given conditions.

Before going into the main experiments, experiment with rotating disks was carefully carried out to supplement and revise the data obtained by other workers. With newly compiled data as reference, intermittence of light by rotating disk was replaced by that of luminescence of the cathode ray tube, and intensity of light and rate of its variation of the former were represented respectively by luminosity and contrast of the latter.

2. Wave form of electric signal

In the television system, light signals from objects are first transformed into electric signals which represent the two-dimensional picture. These signals are then converted to one dimensional function of time and transmitted by carrier waves. In the receiver, the electric signals are transformed back into light signals on the picture tube by horizontal and vertical sweeps, the luminosity of every point of the picture tube being effected by the amplitude of the signal. Every point on the picture tube is irradiated by the electron beam only once for every one field (1/60 s.), but the after-image of the eye and the afterglow of the fluorescence render the image of the object discernible.

With the Benham top, the black and white semi-circles produce alternating stimuli on the retina. If the luminescence of the picture tube is controlled by the

electric signal of frequency corres equal to that of the rotation of the Benham top, the Fechner color is expected to be observed, and because the rotational frequency needed to originate the Fechner color is low which is comparable to the field frequency of the television system, i. e. 60 cps, realization of the Fechner color by television receiver is possible. By this means, detailed study of the Fechner color becomes easy, for, with the electric signal, the frequency can be varied at will with ease.

The stimuli from the Benham top are of considerably complex nature. While spinning, the stimulation proceeds in succession from a black sector to a white sector, to a white sector with black lines, then back to the black sector. To simulate these stimuli by the television picture tube, application of electric signals with the wave form shown in Fig. 16 to the tube will serve. The black portion of the Benham top

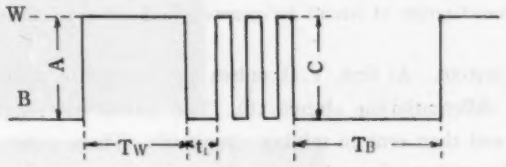

Fig. 16. Wave form of typical Fechner color signal.
W and B stand for white and black respectively.

corresponds to the zero amplitude, and during the time T_B the luminescence of the picture tube is suppressed. The white sector is replaced by the pulse with amplitude A. Thus the contrast is represented by the amplitude. The pulse width T_W corresponds to the center angle of white sector of the Benham top. Changing the ratio of T_W to T_B means changing the ratio between the white and the black sectors of the Benham top, and this changing is very easily done with the cathode-ray tube, but it would be very difficult with the Benham top. Narrow sectors on the Benham top are represented by short pulses as shown in Fig. 16, and electric signals corresponding to various patterns of black circular arcs can be generated by simply varying the phase t_i, varying the number and amplitude C of short pulses and allocating these short pulses at proper intervals. Hence a large number of different electric signals can be produced with least trouble for the study of the Fechner color.

3. Electric signal generator

Electric circuit for producing signals of given wave form is explained in the following.

The arrangement shown in Fig. 17 is for the wave form of Fig. 16. The wave form is made up with vertical driving pulse (V.D.) and horizontal driving pulse (H.D.)

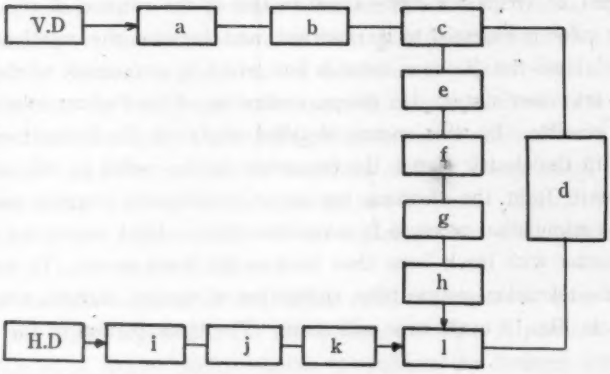

Fig. 17. Blockdiagram of circuit for generation of the wave form of Fig. 16.

of the television system. At first, V. D. pulses are counted by scaling circuit (a) and differentiated by differentiating circuit (b). The pulses are shaped by monostable multivibrator (c) and then sent to mixing circuit (d). These pulses form the highlight signals. The pulses through multivibrator (c) are sent also to differenciating circuit (e) and delayed by an appropriate time in delay circuit (f). These delayed pulses trigger the second monostable multivibrator (h) through differentiating circuit (g).

Short pulses corresponding to the thin circular arcs of the disk are generated as follows: The sine wave from oscillator (i) controlled by the H. D. pulses is shaped by clumping circuit (j) and clipping circuit (k), and gated by signal from the second monostable multivibrator (h) in gate circuit (l). Signals thus fromed are mixed with the highlight signal in mixing eircuit (d), and the expected wave form is obtained.

In short, the wave form can be varied at will by varying the pulse widths, heights and phases of the highlight and short pulse signals and the number of these short pulses.

The wave-form and its electronic circuit panel are shown in photographs 1, 2 and 3.

To investigate whether the condition of background influences the Fechner color, a montage circuit, block diagram of which is shown in Fig. 18, was devised.

A mask signal generator was prepared to inset the Fechner color pattern in any position of the picture with any size and shape. The Fechner color signal is gated in gating circuit (m), the phase of the mask signal is inverted by phase inverter (n), and extracting circuit (o) extracts designed background signal. These signals through (o) and (m) are mixed together by mixing circuit (p), and reproduced on the cathode-

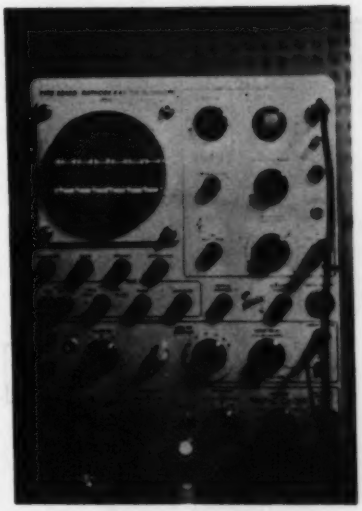

Photo. 1. Wave-form of typical Fechner color signal.

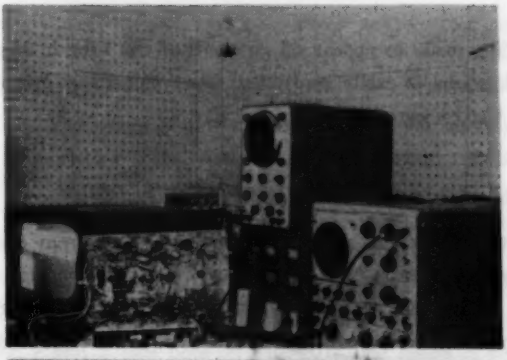

Photos. 2–3. Electronic circuit panel used to generate the Fechner color signal.

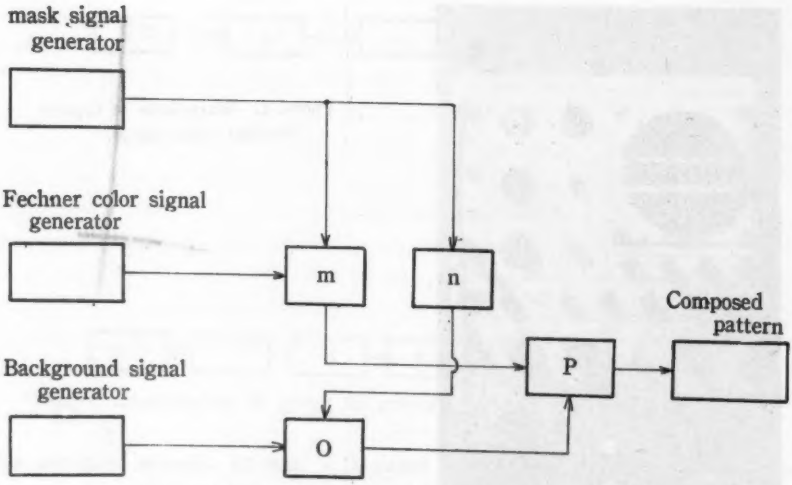

Fig. 18. Block diagram of montage Amplifier.

ray tube. The Fechner color is thus made to appear on any part of the tube in any size, and the brightness of the background is easily controlled. Any pattern or image of moving objects can be used as the background.

4. Experimental Method and Results

A 14 inch television receiver was placed at a distance of 2.5 meters from the observer in a room of o Lux (utter darkness). As the standard condition, the luminosity of the picture tube was set at 10 F. L. and the amplitude of the Fechner color signal at 1.2Vp-p. The Fechner color signal was framed in the area of 20% of the picture tube. The television test pattern (shown in Photo 4) was chosen as the background with its amplitude set at 1.0Vp-p. The phosphor used for the picture tube was type p^4, which is the standard for widely used monochrome picture tubes. This type of phospher is a mixture of zinc sulphide activated by silver and beryllium silicate activated by manganese; its spectrum is a little biased to blue which however did not make much difference in result in comparison with the result of preliminary experiments made on the Benham top illuminated by a tungsten filament lamp, a mercury vapor lamp and the sunlight.

The Fechner color was observed by 14 men and 6 women aged between 12 and over 50, 4 observers each in the teens, twenties, thirties, fourties and fifties. Among these 20 observers, one half had no previous experience on the Fechner color.

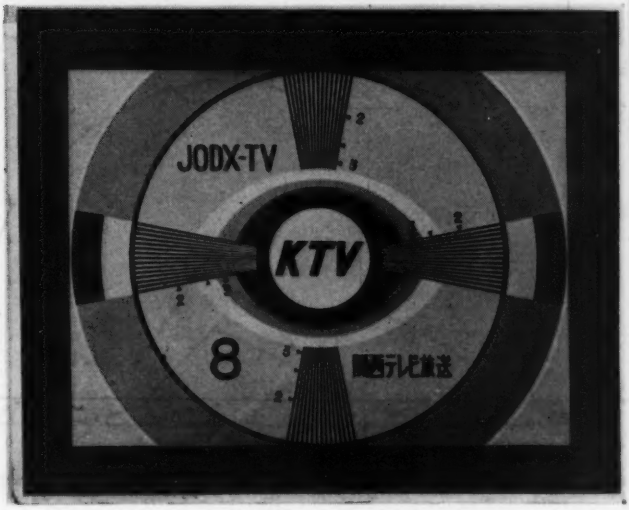

Photo. 4. TV. Test pattern.

Experiment 1

The range of tint of the Fechner color and the color-sensation were investigated. The picture tube was set at the standard condition described above. The Fechner color signals of different wave forms and repetition frequencies were applied, and the color-sensation of each observer was recorded by comparing it with the color table.

The maximum color-sensation for each hue was, 2.5 RP 4.0/7.0, 5.0 P 3.0/10.0, 8.3 PB 7.0/5.7, 6.5 B 7.5/4.2, 2.3 BG 8.0/3.7, 2.5 G 8.0/3.5, 7.3 YG 7.3/2.8, 5.7 Y 9.0/4.0, 5.0 RY 7.5/5.0.* The color-sensation was graded on the basis of these colors as 5, 4, 3, 2 and 1. (see note on Fig. 20) The result is shown graphically in Fig. 19. The hues which could be observed by the present apparatus were RP, P, PB, B, BG, YG, Y and RY. The hues RP and P were most vividly observed. Except RY, majority of the observers perceived the colors.

The graphs in Fig. 20 show how different hues are perceived by the observers. Since 5.0 P was perceived very distinctly by all the observers, this hue was taken as the standard for determining the brightness and saturation of the Fechner color produced under different conditions.

---

* The color representation is by H. V/C of Mansel color system where H is Hue, V is Value (or brightness) and C is Chroma (or saturation).

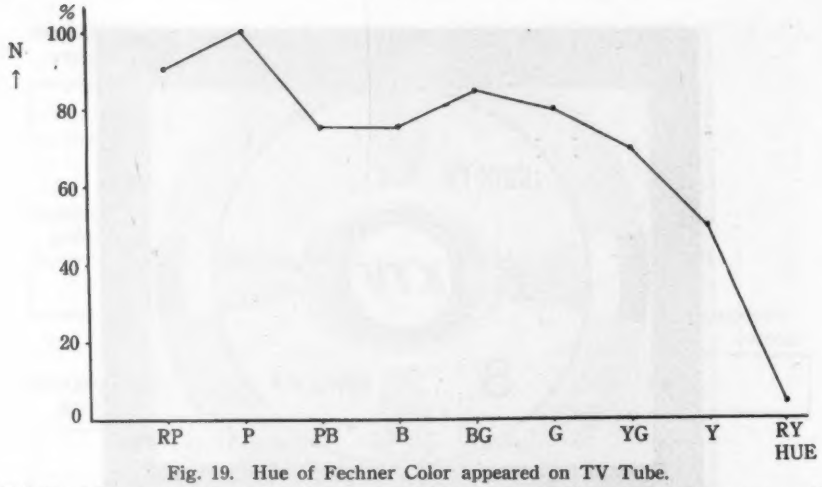

Fig. 19. Hue of Fechner Color appeared on TV Tube.
N is the percentage of observers who perceived the color. Total number of observers was 20.

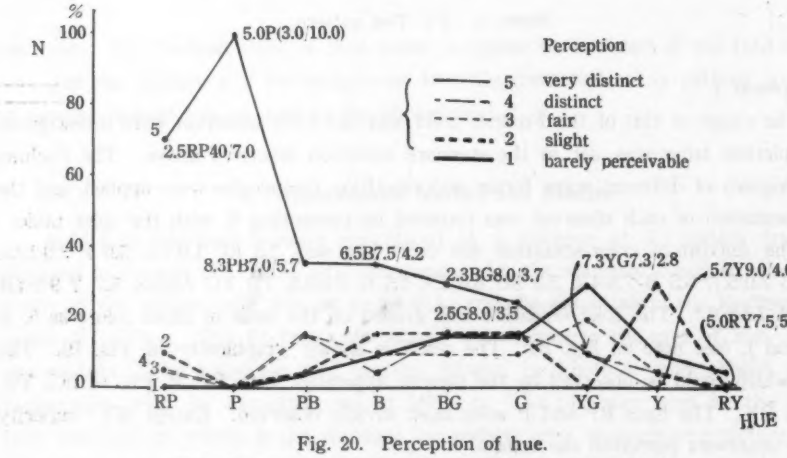

Fig. 20. Perception of hue.
N is the number of observers in percent of the total.

Experiment 2

The effect of amplitude of the intermittent light stimuli on the Fechner color was investigated with 5.0 P signal. Brightness and saturation of 5.0 P hue were observed by varying continuously the signal amplitude from 0.4 Vp-p to 1.2 Vp-p then back to 0.4 Vp-p by 0.2 Vp-p steps with the results shown in Figs. 21 and 22. When the signal amplitude was reduced below 1.0 Vp-p, the saturarion decreased

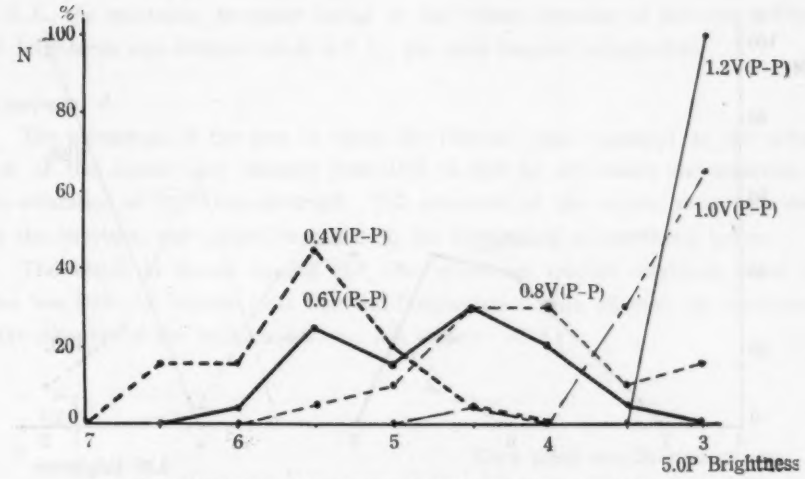

Fig. 21. Dependence of brightness of color on color signal amplitude.

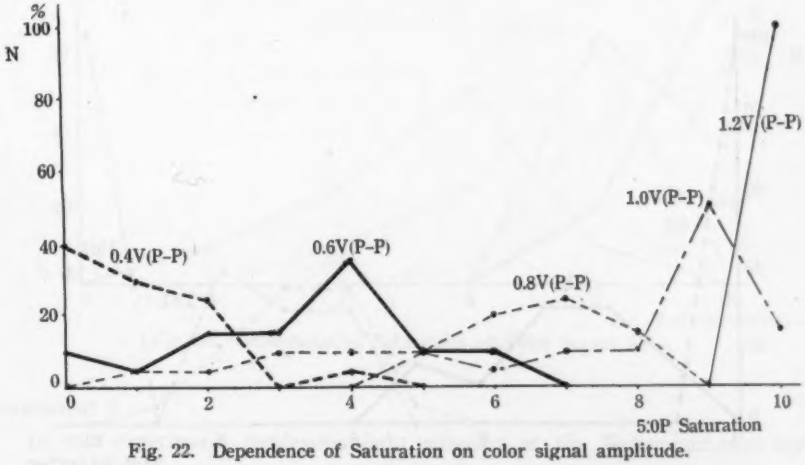

Fig. 22. Dependence of Saturation on color signal amplitude.

and the brightness increased both suddenly, the color becoming difficult to be discerned, and when reduced further below 0.4 Vp-p, there was only the flickering of white light, the color becoming indiscernible. Amplitude of above 1.2 Vp-p saturated the brightness, hence during the experiment, the amplitude was set below this value.

Experiment 3

The brightness of the picture tube was varied from 4 F. L. to 12 F. L. then back

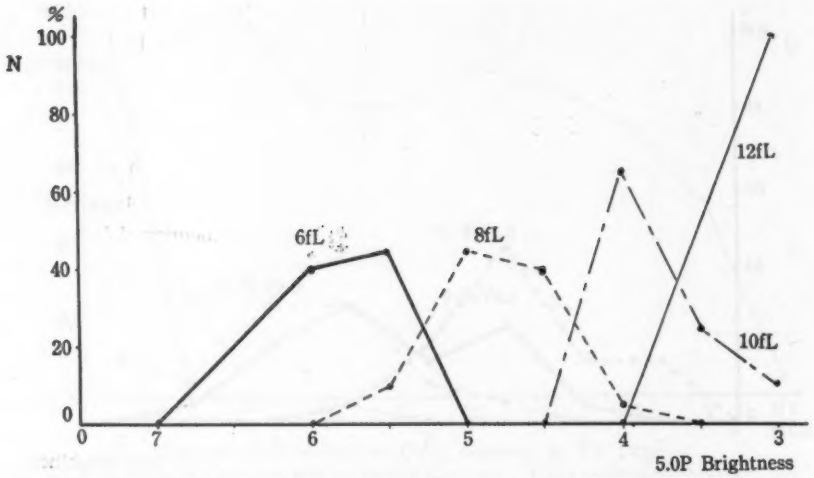

Fig. 23. Dependence of Brightness of Color on Brightness of Picture tube.

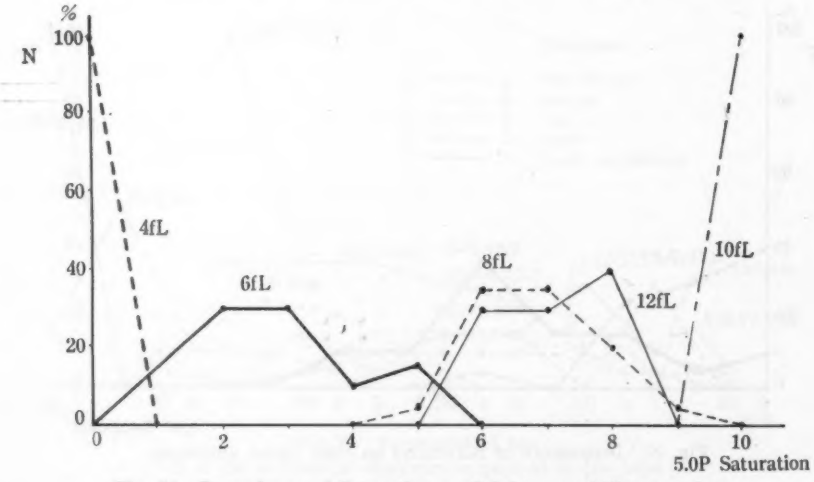

Fig. 24. Dependence of Saturation on Brightness of Picture tube.

to 4 F.L. by 2 F.L. steps, and the relations of the total light stimulus to the brightness and the saturation of the Fechner color with 5.0 P signal was investigated. The results are shown in Figs. 23 and 24. The brightness of 5.0 P increased with the brightness of the picture tube, and the saturation reached maximum when the brightness of the picture tube was 10 F.L. When the brightness was increased to

12 F. L., the saturation decreased owing to the relative decrease of stimulus. When the brightness was reduced below 4 F. L., the color became indiscernible.

Experiment 4

The percentage of the area in which the Fechner color appeared to the whole area of the screen was changed from 10% to 50% by 10% steps, and variation of the saturation of 5.0 P was observed. The remainder of the screen area was used for the television test pattern representing the background as mentioned before.

The result is shown in Fig. 25. The saturation reached maximum when the area was 20%. It became clear that the Fechner color was affected by continuous light stimulus of the background.

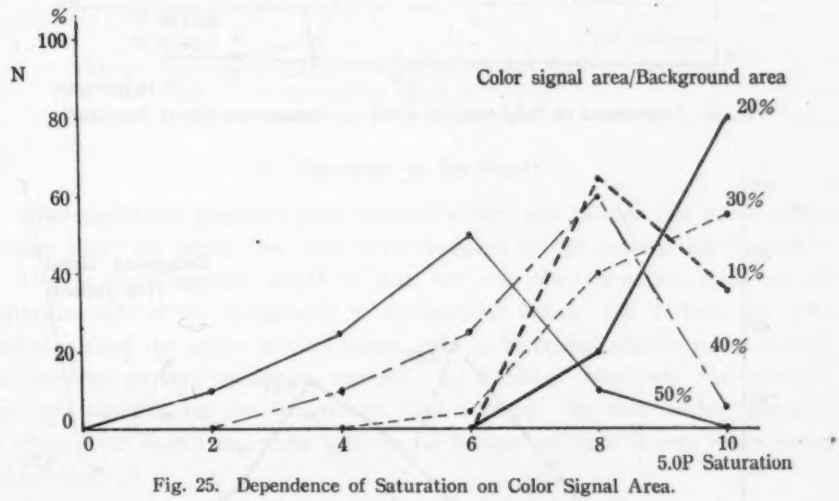

Fig. 25. Dependence of Saturation on Color Signal Area.

Experiment 5

In this experiment, continuous light stimulus of the background was varied. Amplitude of television test pattern signal of the background was varied from 0.2 Vp-p to 1.0 Vp-p by 0.2 Vp-p steps, and the saturation and brightness of 5.0 P were observed.

The results are shown in Figs. 26 and 27. Brightness and saturation of the Fechner color were much affected by the condition of the background.

Experiment 6

The effect of the background was further investigated. Effects of different

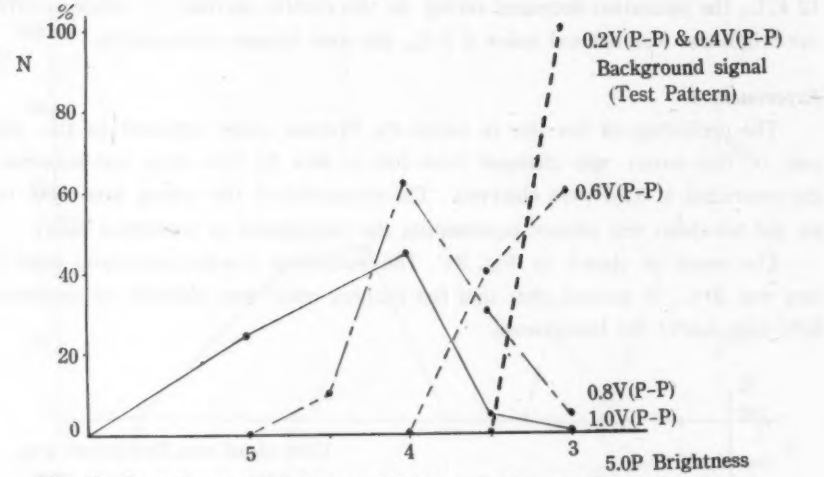

Fig. 26. Dependence of Brightness of Color on Background Signal Amplitude.

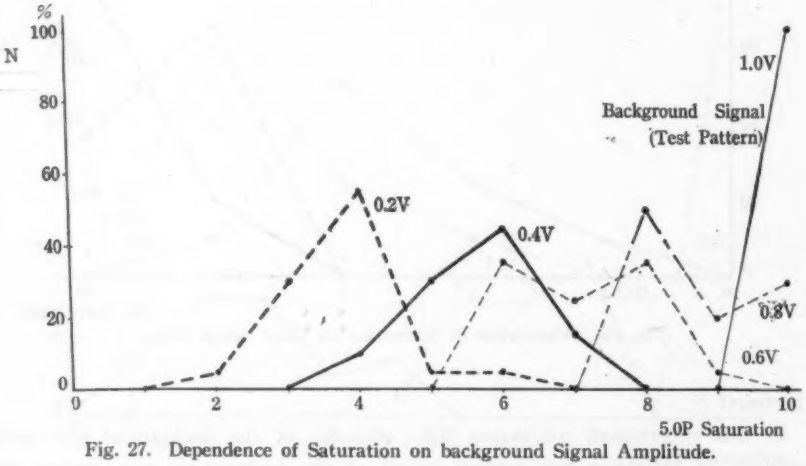

Fig. 27. Dependence of Saturation on background Signal Amplitude.

background patterns—television test pattern, striped pattern, gray scales of seven grades, image of moving objects taken by a image orthicon camera, and moving pictures by cinefilm—on the saturation of 5.0 P were observed. The amplitude of all these background pattern signals was set at 1.0 Vp-p, but their light stimuli differed.

The result is given in Fig. 28 which shows that, in the study of the Fechner color effect of the background should not be ignored.

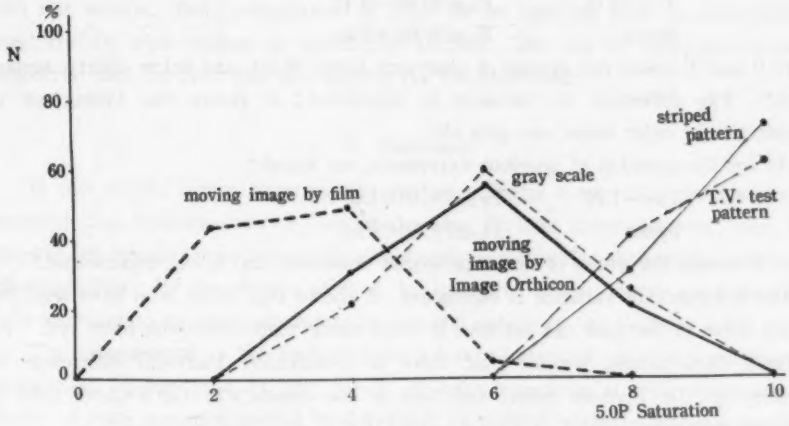

Fig. 28. Dependence of Saturation on Background Pattern. Amplitude of background signal is 1.0vp-p.

5. Discussion on the Results

The experiments described above revealed several new factors that influence the Fechner color—the factors that could never be found by the rotating disk method.

One of the important results is that, not only the intermittent light but the continuous light of the background is an essential factor. The cathode ray tube method enabled the nature of the Fechner color to be studied objectively by varying the involved physical quantities, especially by varying collectively the intermittent light stimulus and the background light stimulus. By this method, intensity of intermittent light, total light stimulus, or background light is very easily varied independently.

Let us begin the discussion with the range of tint of the Fechner color.

Difference in perception for all the hues, found among the observers of different sexes and ages and between those who were experienced in the Fechner color and those who were not, is examined in the following.

As for the sexes, we found

$$F_{MW}=1.06, \qquad F_{0.05}(111,47)=1.53$$

hence $$F_{0.05}(111,47)>F_{MW}$$

where M and W mean the group of men and the group of women respectively.*

Thus the difference in variance is not significant, and no difference is apparent between the sexes. As for the ages, the observers are devided into two groups, above thirty and below thirty.

$F_{0Y}=2.11$, $F_{0.05}(95,63)=1.47$

hence $F_{0.05}(95,63)<F_{0Y}$

where 0 and Y mean the groups of observers above thirty and below thirty respectively.* The difference in variance is significant; it shows the falling off of perceptivity for color when one gets old.

As for the question of previous experience, we found

$F_{NE}=1.76$ $F_{0.05}(79,70)=1.45$

hence $F_{0.05}(79,79)<F_{NE}$

where N means the group of non-experienced observers, and E the experienced.*

The difference in variance is significant; it shows that those who have seen the Fechner color in the past can perceive it more easily than those who have not.

From these result, we see that there is considerable individul differences in perception of the Fechner color, and this is one reason why the Fechner color is called the subjective color.

However, as far as 5.0 P is concerned, whole observers perceived it with equal ease. Therefore, if we used 5.0 P as the standard and vary the brightness and saturation of the Fechner color, we should except to find the same tendency for all the observers regardless of sex, age and experience in increase or decrease of color-sensation. This is evidenced by the example shown in Table 1. This tendency is considered to be univarsal.

Table 1.

	brightness	saturation
sex	$F_{MW}=1.59<F_{0.05}(51,21)=1.93$	$F_{MW}=1.06<F_{0.05}(69,29)=1.74$
age	$F_{0Y}=1.47<F_{0.05}(31,41)=1.79$	$F_{0Y}=1.29<F_{0.05}(39,59)=1.64$
experience	$F_{NE}=1.34<F_{0.05}(33,39)=1.80$	$F_{NE}=1.27<F_{0.05}(49,49)=1.61$

The Fechner color for producing purple hue was once given on television broadcast waves. According to reports that were received, the hue was noticed on many private television receivers, which furnished useful information that the Fechner color is real.

Instead of the electronic circuits with a cathode ray tube, a special cinefilm was prepared for generating the Fechner color signal and tried on a television receiver

* F_{AB} is the inverted beta (F) function for the two groups A and B; $F_{0.05}$ is the value of the function for $\alpha=0.05$; the numbers in the blacket are the degrees of freedom for the groups A and B respectively.

with fair results. But, preparation of films to be used to vary several different conditions in wide ranges is technically limited. The use of electronic circuit is considered still the best way of studying the Fechner color.

6. Summary

In this article, a new experimental method utilizing a television picture tube for studying the Fechner color is described. The Fechner color has not been fully investigated because it is being regarded merely as a singular phenomenon concerning color-sensation. By the present method, it is possible to vary every condition of the light stimulus to inquire systematically into the nature of the Fechner color.

The phenomenon of the Fechner color is a very important one that needs thorough explanation in the field of the theory of color especially of color-sensation. The theory of color-sensation should be developed in parallel with the advance of physiology, but first of all one must be fully acquainted with the color phenomenon in the field of physics. The present experiment is believed to be a step to further the study of the color-sensation.

The author wishes to express heartfelt thanks to Prof. Yoichi Uchida, University of Kyoto, Dr. Ryuzaburo Taguchi, Science of Color Society; Prof. Kazunori Yuasa, Konan University, for their constant guidance and valuable suggestions.

References

1. M. B. Erb and K. M. Dallenbach, Subjective colors from Line Patterns Cornell University (1935).
2. S. Moskowitz: *Pulse Techniqnes.* (The Prentice-Hall Co. Inc. New York 1951).
3. F. E. Terman: *Electronic Measurements.* (The Mcyraм-Hill Book Co. Inc. U.S.A. 1952).
4. Ryuho Kaneko, Psychology of Vision of Television (in Japanese) the Journal of the institute of Television Engineers of Japan **12** (1958) 367.
5. Hisao Kabayama, Physicology of eye in Television (in Japanese) the Journal of the institute of Television Engineers of Japan **12** (1958) 315.
6. Masami Yamada, The Fluorescence of a Cathode-Ray Tube. (in Japanese), Broadcast Engineering **3** (1950) 411.
7. Yukihiko Harai, The Fechner Color by various disk (to be published).
8. Yukihiko Haral, Physical Construction of Color-sensation with Fechner color (to be published).